College of Engineering
Department of Meteorology and Oceanography

Technical Report

An Attempt to Use Satellite Photography in Numerical Weather Prediction

James H. S. Bradley
Christopher M. Hayden
Aksel C. Wiin-Nielsen, Project Director

Supported by:

Environmental Science Services Administration
Contract Cwb-11145
Washington, D. C.

TABLE OF CONTENTS

TABLE OF CONTENTS (concluded)

LIST OF TABLES

LIST OF FIGURES

LIST OF FIGURES (concluded)

ABSTRACT

TIROS photographs were used for barotropic reanalysis in the Pacific, changes in the stream function or its Laplacian being advected into areas with verification data by the NMC barotropic model, following McClain, Ruzecki and Brodrick. No significant forecast improvement was obtained in cases of unusually bad forecasts, despite experiments in varying the intensity of the reanalyzed systems. No continuity and no radiation data were available: the estimation of winds and vorticities is difficult. Hindcast-reforecast procedures indicated that the main causes of error in unusually bad forecasts are not susceptible to satellite correction, and that difficulties in the balance equation had caused the stream field to contain many negative absolute vorticities not present in the geopotential analysis. The methods used would be more promising in cases with smaller forecast errors.

1. INTRODUCTION

1.1 Purpose

It has been recognized for several years that the problems of forecasting over and on the eastern sides of large oceans might be alleviated by using satellite photographs to improve the analysis by means of inferences about the fields of horizontal and vertical motion, temperature and humidity. A large sample of such papers can be found in almost every issue of the Monthly Weather Reivew for several years past. Rapid electronic computers have long been in routine use for large scale hydrodynamic forecasting: (see Thompson (1961), and Kibel (1963)). The integration of satellite data into such hydrodynamic schemes appeared to us a promising line of inquiry, although at present, modifications have been made only to the output from an automatic machine analysis program. We have studied selected cases in which according to the Meteorological Satellite Center operational barotropic and baroclinic models gave unusually bad forecasts, using the techniques of McClain, Ruzecki and Brodrick (1965) to infer the stream, vorticity and vorticity advection fields from TIROS photographs when significant differences from NMC analyses appeared to exist over the Pacific Ocean.

1.2 Method

Either the 500 mb stream field or the 500 mb Laplacian field was reanalyzed by the methods and using the programs of McClain, Ruzecki and Brodrick (1965). Since the few available conventional data were preserved (and conventional data which arrived too late for the NMC analysis introduced), it was necessary to forecast by the NMC barotropic model for some period, chosen as 36 hours, in order to propagate the modifications into another region where at least some verification data exist. Attention was directed to the quantitative assessment of the effects of changes in the intensity of the reanalyzed system.

Further attempts were made to hindcast by a barotropic model without mountains or friction in order to elucidate how far the analysis required for a correct forecast might be ascertainable from satellite data. The numerical analysis problems of weather analysis and forecast models were investigated only in so far as improvements to them appeared likely to remove complications which masked changes due to satellite reanalysis.

The verification programs of McClain, Ruzecki and Brodrick (1965) were used, plus verification in terms of zonal harmonics of the stream function in order to examine

separately those scales of motion which can be modified by the application of satellite data.

2. REANALYSIS PROCEDURES

2.1 Basic maps

Five basic maps were printed from the NMC data tape for use with the reanalyses. These were: 500 mb heights, 500 mb streams, -12 hr 500 mb streams, 1000-500 mb thickness and 650 mb vertical velocity. These maps, in conjunction with the radiosonde data, were used in investigating the structure of the thermal advection and vertical velocity fields in the original NMC analysis. These permit some subjective analysis of the probable cloud formations prior to modfying the stream field or the vorticity field to more closely comply with the satellite photographs.

2.2 Radiosonde Data

A program was prepared to extract conventional and bogus data from the Automatic Data Processing file of the NMC input tapes over any given grid rectangle or latitude-longitude sector. Station names were added from a look-up table. Listings of temperature, potential temperature, dewpoint, observed wind, D-value (height minus standard atmosphere height) and temperature advection (from the thermal wind equation) are made for all mandatory and significant temperature levels, and P-T diagrams and

tephigrams with automatically interpolated lines prepared for all radiosonde observations with enough levels.

One seriously defective observation incorporated in the NMC analysis was found for 0000Z 26 January 1964; other spurious points found appeared to have been excluded.

The Northern Hemisphere Data Tabulations were used to supplement the ADP file with late data.

2.3 Vorticity

Vorticity maps referred to here are grid point calculations of the five point finite difference stream Laplacians. The relative vorticity and vorticity advection are then written as:

$$\xi = \nabla^2\psi = \frac{m^2 g}{d^2 f_o} \nabla^2 \hat{\psi}$$

$$V \cdot \nabla \xi = \frac{m^2 g^2}{4d^4 f_o^2} J(m^2\nabla^2\hat{\psi}, \hat{\psi}) \simeq \frac{m^4 g^2}{4d^4 f_o^2} J(\nabla^2\hat{\psi}, \hat{\psi})$$

where ψ is the stream function, $\hat{\psi} = \frac{f_o}{g}\psi$, J is the Jacobian, $m = (1 + \sin 60)\,(1 + \sin\phi)^{-1}$ is the map factor, f_o is the Coriolis parameter at latitude 45^oN, d is the NWP grid distance of 381 km. Printed maps are given as $\nabla^2\hat{\psi}$ and $J(\hat{\psi}, \nabla^2\hat{\psi})$ in meters and meters squared respectively. In the following, the terms "vorticity" and "Laplacian" are used interchangeable to refer to the field of $\nabla^2\hat{\psi}$.

The philosophy underlying modification of the vorticity is fully discussed by McClain et.al. (1965). In essence, the cloud patterns viewed in the satellite photographs are assumed to be allied with areas of positive vertical velocity. This in turn is related to the vertical variation of the vorticity advection and horizontal Laplacian of the thermal advection. Since the latter terms are frequently additive, rather than compensatory (Pfeffer, 1962), and since a barotropic forecast model has been used, it is the normal practice to modify the vertical velocity field by variations in the vorticity field. It is apparent that this cannot be executed without some difficulty. Modifications of the vorticity field alter the vorticity advection, but the effect is only apparent after the new stream field is obtained by relaxation.

A second complication with reanalyses of the vorticity field is that there is no way of preserving observational data in close proximity to the reanalysis as it is impossible to predict the final form of the relaxed stream field. The difficulty can be circumvented only by restricting the size of the reanalysis area.

A further difficulty of the vorticity reanalysis is the requirement that the total relative vorticity be conserved in any modification. Failure to comply with this

restriction results in a relaxation stream field which evidences changes far outside the limits of the reanalysis area. The same effect is observed if the vorticity modifications are sufficiently severe, but it is minimized through the conservation principle. This restriction places a considerable restraint on the subjectivity of the reanalysis and is quite time-consuming in terms of operational SINAP modifications. For this reason, and those mentioned above, the majority of the work done under this project concerned stream-line reanalysis.

2.4 Stream function

Stream fields are printed as $\hat{\psi}$ with the symbol defined as above. Consequently the field is in meters. Modifications of the stream field are more straightforward than those of the vorticity as the analyst is able to apply directly his knowledge of cloudy regions as related to wave patterns in the atmosphere. The integrity of the stream function modifications in conforming with the vorticity field is easily checked, though care must be exercised that negative absolute vorticities are not introduced. This problem occurred repeatedly on this work but only because the magnitudes of the stream function alterations were very large. It is unlikely that smaller changes

would have the same effect.

2.5 Estimation of Vorticity and Wind

While the positioning of stream or vorticity field modifications has been investigated quite broadly in the literature, the magnitude of such changes has understandably received little attention. The satellite photograph provides no information concerning the primary atmospheric variables, nor, beyond some subjective interpretations, is it possible to determine the heights of the systems revealed by cloud formations. In all probability future work with satellite radiation data will alleviate these difficulties, but the work under this project was carried out solely with the cloud photographs.

In essence, the analyst is guided by the available conventional data in the region of satellite coverage, wind direction estimates from the cloud photographs (Widger et.al.), persistence of systems recently over data dense areas, and climatology of the region. Beyond these aids, the magnitude of modifications is completely subjective. In an attempt to introduce some objectivity into the reanalysis procedure, considerable effort has been expended in an empirical study of the effects which variations in

magnitude of the modifications have on the forecast stream field. The results from this study of a single case cannot be considered general, but they certainly give an indication of the sensitivity of the reanalysis procedure.

2.6 Energetics

We have assumed that the systems present in our reanalysis waves are similar to those known in areas of dense observations, i.e. that the barotropic and baroclinic mechanisms discussed by McClain, Ruzecki and Brodrick (1965) are dominant. A scale analysis by the method of Kibel (Chapter 3) suggests that this is valid even for the system of 5 November 1963.

In order to influence the forecast significantly the meteorologist is both justified and obliged to draw conclusions about larger structures and scales of motion than are directly visible on the isolated swaths we have used. This extension has been made according to accepted synoptic principles.

3. VERIFICATION

3.1 Change Correlation Coefficient, RMS Error, Error Maps, Forecast Improvement Chart

Verification of the improvement introduced by modifications in the analyses can be at best only tentative. The procedure utilized here follows that of the Satellite Laboratories in running numerical forecasts from both the NMC and SINAP initial stream fields. The 36 hour forecast fields are then compared with the NMC analyzed field for that time. Two problems are immediately apparent. Firstly, since the forecast model is barotropic, no initial modifications can correct baroclinic development. This problem is obviated by choosing for study only those cases where we are told that error charts derived from NMC barotropic and baroclinic forecasts both show large discrepencies from the observed state. This suggests that the failure of both forecasts may be due to poor specification of the initial state rather than baroclinic development. Secondly, and more importantly, the procedure assumes inherently that the NMC analysis at the forecast time is itself accurate. Since the analysis is derived from a previous forecast modified by observation, the analysis in all likelihood is biased to the previous forecast, at least in areas of sparse data. The verification analysis itself is thus suspect, particularly for those

cases where SINAP modification produces forecast changes which are in sparse data regions. This problem is evidently dependent on the scales of the systems involved. Even if it were possible to delineate the smaller systems from the satellite coverage, it is doubtful that improvements could be recognized in the verification statistics. It may be concluded that the modifications must be applied to the larger systems.

The statistical verification procedure used in the reanalysis program at the Satellite Laboratories was used without modification. Root mean square errors and correlation coefficients were calculated from the NMC and SINAP barotropic forecasts for the following fields: stream function, vector geostrophic wind, stream Laplacian and stream Jacobian. More specifically, difference fields were utilized. For example with the stream field, the parameters from which the statistics were computed were: NMC forecast minus NMC initial field; NMC verification minus NMC initial field; and SINAP forecast minus SINAP initial field.

In addition to the verification statistics two difference charts were computed for the forecast stream fields. These were: NMC forecast minus verify; SINAP forecast minus verify. Finally a forecast improvement chart was obtained

by subtracting the absolute magnitudes of the difference charts at each grid point. These charts permit detailed analysis of the point by point changes effected by the SINAP modifications. Computations were made over both the entire NMC 2329 grid and a subgrid which was determined to include only the region significantly affected by the reanalysis.

3.2 Zonal Harmonic Analysis

The idea of analysis in zonal harmonics or any other orthogonal functions is to examine certain scales of motion separately; in this case, the zonal wavenumbers of the order of 12 in which modifications are made by the analyst. The corresponding weakness of harmonic analysis is that it diverts attention away from the meteorological system (wave-group) visible on maps; harmonic analysis is most useful when the waves used have some almost autonomous existence and motion over the period studied, or when barotropic or baroclinic interactions are conveniently describable in terms of them.

Zonal Fourier analyses of the stream field in terms of sines, cosines, amplitudes and phases of wavenumbers 0-15 were made at 5 degree latitude intervals from 20°N to the pole. The effects detected were large enough to indicate

that no further significant information would be obtained for our restricted verification purposes, by more refined analyses in terms of surface harmonics, Gram-Schmidt grid orthogonal functions, or eigenvectors of the relaxation matrix used in the barotropic forecast. Analysis of the zonal mean stream function directed attention to changes in the zonal mean wind profile, as well as to changes in the hemispheric mean stream function caused by the boundary condition of the balance equation. This cannot radically alter the evaluation of forecasts when the wind verification is poor, but it should be allowed for in calculating the RMS errors and correlations of changes in the stream function.

4. HINDCAST - REFORECAST TECHNIQUE

4.1 Removal of Mountains and Friction

It was decided to prepare hindcasts from the verification data to the initial time in order to elucidate how far errors of analysis might be correctable by satellite data. First attempts rapidly overflowed in the mountain and friction terms, so they were deleted. Reforecasts to the verification time were prepared in order to cast light on the truncation error of this process. Mean and maximum forecast improvements for 5 November and 26 January were 46 and 53, and 183 and 333 meters repectively; and maximum errors were 111 and 201 meters respectively.

The NMC barotropic forecast program and balance equation make the following approximations:

1. The initial stream field is equal to the geopotential around the edge.
2. The tendency at the edge is zero.
3. The mean tendency over the whole grid (equally weighted for each point) is subtracted from interior points only.
4. The smoother does change edge points slightly: we applied the smoother at every twelvth time step.
5. Negative absolute vorticities are set to zero but the associated stream fields are not changed.

Tables 5.1 and 6.2 give some Fourier coefficients from these processes.

4.2 Conclusions

It is clear both from the Fourier coefficients and from the maps that a substantial part of the error cannot be significantly influenced by isolated swaths of satellite photographs: much of it cannot be error in the initial analysis. In particular, the profile of the zonal mean required (hindcast) and observed shows differences up to 63 meters, and the required profile shows a greater pole-to-equator gradient. Wavenumber 1 shows little resemblance, and wavenumbers 2-15 no resemblance for 26 January 1964.

On the other hand, the reforecasts also leave a good deal to be desired. While the mean forecast improvement (as defined by McClain, Ruzecki and Brodrick (1965) is 46 meters for 5 November 1963 and 53 meters for 26 January 1964, errors remain of 111 meters and 201 meters respectively. Around the edges differences reach 7 and 18 meters respectively, due to the smoother.

4.3 Computational Instability

The suspicion of non-linear computational instability

arose from a hindcast-reforecast from 1200Z 27 January 1964 to 0000Z 26 January 1964 and back, which was by far the worst of all the forecasts produced. Errors attained 450 meters, and an intense zonal jet replaced the strong block over the west coast of North America. The linear stability criterion (Knighting, 1962) was met in all cases by a factor slightly less than two.

The hindcast was repeated with the over-relaxation coefficient a pre-determined function of time, and with a diagnostic record tape (Appendix B): the two hindcasts bore no resemblance to each other.

The hindcast was again repeated with half-hour time steps, and with the smoother applied at every twelfth step: the over-relaxation coefficient was a pre-determined function of time. The change in the time step made comparatively little difference to the hindcast, and the explanation of this fact is unknown.

Forecasts with the over-relaxation a function of time, with a diagnostic tape, and with half time steps were run from 0000Z on both 5 November 1963 and 26 January 1964 to 1200Z the following day. It was concluded that computational instability was not a large factor in either of these cases, in the classical sense that the solution goes to infinity; yet it is clear from the Fourier analyses of the hindcast-reforecast results that truncation errors and the irreversible

effects of the smoother and the zeroing of negative absolute vorticities introduce significant approximations.

4.4 Negative Absolute Vorticities

The diagnostic program (Appendix B) prints the I,J and latitude-longitude location of each negative absolute vorticity and its ratio to the local Coriolis parameter.

Ninety-two negative absolute vorticities occur in the original NMC stream field for 0000 GMT 26 January, with the largest ratio -.747f at 42,7 or 19.8°N 124.2°E. Of these, 29 are south of 20°N and 44 between 20°N and 30°N. One lies at 32,43 or 35.6°N 76.4°W on land near Cape Hatteras. At 0000 GMT 5 November 1963, 18 of the 55 are south of 20°N, 28 between 20°N and 30°N, and the largest ratio is -.567f at 23,47 or 18.8°N 53.4°W.

A diagonal pattern is well marked (Table 4.1) and some triple groups suggest erratic high points in the stream field as though much short wave noise were present. Knighting (1962) gives the criterion for ellipticity of the balance equation as approximately that the absolute vorticity must exceed f/2; hand examination of a dozen points in the original geopotential field which had negative absolute vorticities in the stream field suggests that about a third of these points

violate the criterion for ellipticity. No points of negative absolute vorticity were found in this sample of the geopotential field.

During the forecast points of negative absolute vorticity usually intensify and propagate downwind, sometimes attaining -2.5f. There is no apparent relation to the persistent points of slowest convergence. The smoother weakens them all and removes some. In view of the slight changes in the forecast caused by halving the time step (section 4.2), with the smoother applied at every twelfth step, it is unlikely that negative absolute vorticities as such greatly influence the cases studied. The ridge and trough positions in the stream and geopotential fields largely coincide, but we have not computed the geostrophic vorticity and momentum transports.

I	J	Ratio	I	J	Ratio
26	3	.144	27	4	.082
28	5	.258	29	6	.181
42	7	.747	43	6	.568
44	5	.070	45	6	.234
46	7	.125	47	8	.498
48	9	.535	49	10	.509
50	11	.422	51	12	.272
51	17	.284	50	18	.441
49	19	.109			
44	44	.165	45	45	.407
44	46	.522			
16	36	.135	17	37	.176
16	38	.030			

TABLE 4.1

Illustrative Locations of Negative Absolute Vorticities and Ratios to the Local Coriolis Parameter. NMC Stream Field, 500 mb, 0000Z 26 January 1964.

From the stream and geopotential fields given on the NMC tapes, the complete balance equation is not satisfied by amounts approaching 100% even at points where the terms are individually large; including points at which the stream field has negative absolute vorticity. While we do not know what smoother is used in the operational balance equation, in our opinion further clarification of this matter is advisable if further studies are made on cases of unusually bad forecasts.

Although the operational barotropic model sets negative absolute vorticities to zero while leaving the associated stream field unaltered, we calculated the implied stream field by the usual relaxation used in Laplacian reanalysis. All changes were negative, the hemispheric mean cyclonic vorticity having been increased; the form is a rough egg shape with a maximum change of 142 meters at 50°N 130°W for 0000GMT 26 January 1964. For 0000 GMT 5 November 1963 two maxima appear, with no apparent relation to forecast errors. While the hindcast-reforecast procedure indicates a stronger zonal wind as one feature of the analysis necessary for a correct forecast, and while the relaxation of negative absolute vorticities appears to move in the right direction, it is known that zero absolute vorticity is not the correct value.

5. CASE OF 5 NOVEMBER 1963

5.1 Nature of the System

The visible cloud mass (TIROS 7, orbit 2046) suggesting a departure from the NMC analysis lay near ship 4YP, with a size of about 5 degrees (2 grid lengths; wavenumber 72) zonally and 10 degrees meridionally. No indication of its presence was found in the radiosonde sounding at 4YP, and it was concluded that the surface cyclone was probably small and incipient. It is, however, permissible to infer a larger structure similar to that commonly found in areas of minor cyclogensis. Consultation of all surrounding conventional reports did not suggest that any reanalysis should exceed wavenumber 12, although it was considered that in view of the smoothing used in the barotropic model components at wavenumbers greater than about 15 had little prospect of significantly influencing the forecast.

The lapse rate at 4YP is near dry adiabatic to 850 mb, and near wet adiabatic but far from saturated to 500 mb. The sounding at Cold Bay (55°N, 163°W) shows a definitely warmer airmass above 530 mb. (-31°C at 500 mb., as against -36°C at 4YP). The wind direction at 4YP is constant with height. Thus the wave can be only minor, with no thermal support for strong baroclinic development, and not of a type specifically associated with substantial long wave motion.

5.2 Origins and Energetics of Such Systems

According to the scale analysis of Kibel (Chapter 3), for a system of 500 km size the inertial terms in the equations of motion are in the order of 20% of the Coriolis term. Nor is it likely that much will be known observationally of such small systems except from the frequent satellite coverage which has just become available. It was concluded that in practice one can do no better than follow the energetic assumptions of McClain, Ruzecki and Brodrick (1965).

The small wave observed of 5 November 1963 may probably be treated as a stable barotropic wave in a region of approximately zonal flow. The question which may be asked is what larger scales of motion are implied by the occurrence of such a wave.

5.3 Errors of the Forecast

The error chart for the JNWP forecast showed errors up to about 190 meters, and the pattern of positive and negative areas indicated substantial contributions from zonal wavenumbers five and six, which were documented by Fourier analysis in Table 5.1. It was noted that these are the baroclinically active waves, but no use can be made of this fact within the confines of a barotropic investigation. The reanalysis made

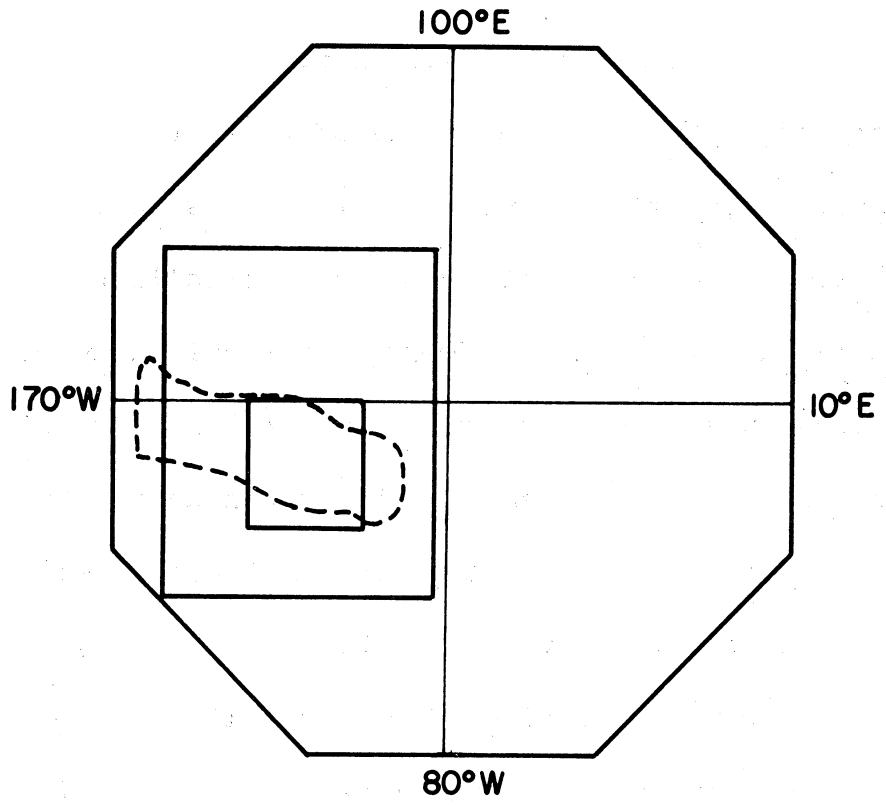

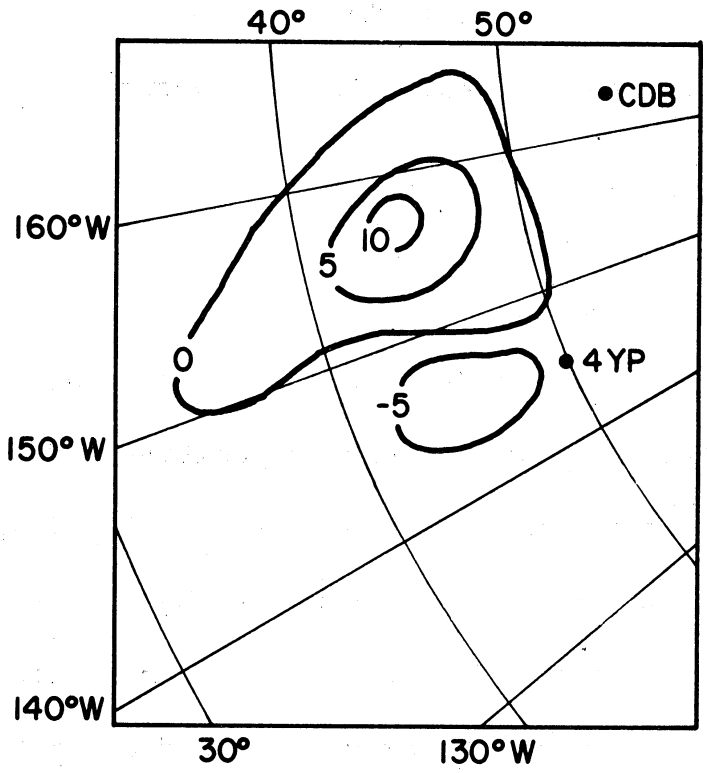

Figure 5.1. Above: Reanalysis area (interior rectangle) and verification subarea for case of 5 November 1963. Dashed line indicates coverage by TIROS 7 orbit 2046 for 1934GMT 4 November. Below: Laplacian change field for 0000GMT 5 November 1963. Units are in tens of meters.

by the Meteorological Satellite Laboratories and rerun on our computer gave similar results, identical to those obtained on the NMC machine, with forecast improvement up to 80 meters but with just as large errors remaining. No significant change resulted from our reanalysis.

5.4 Reanalysis

Three Laplacian reanalyses were made, the first two being rejected as showing meteorologically implausible systems. In the third (fig. 5.1), maximum changes of -69 meters and +111 meters at 45°N and with a zonal separation of 10° gave a trough and ridge separated by 15° (zonal wavenumber 12 for a whole wave) in the stream function change map (fig. 5.2). The grid resolution is a limitation on reanalysis on this scale. Small changes were implied in longer waves. The Coriolis parameter corresponds to a Laplacian of 130 meters.

5.5 Verification

No significant change in correlation coefficients or RMS errors resulted from this reanalysis. The maximum forecast improvement attained 56 meters in an area of large errors over the western United States, but errors of 190 meters remained (fig. 5.3). Although forecast deprovements reached only 20

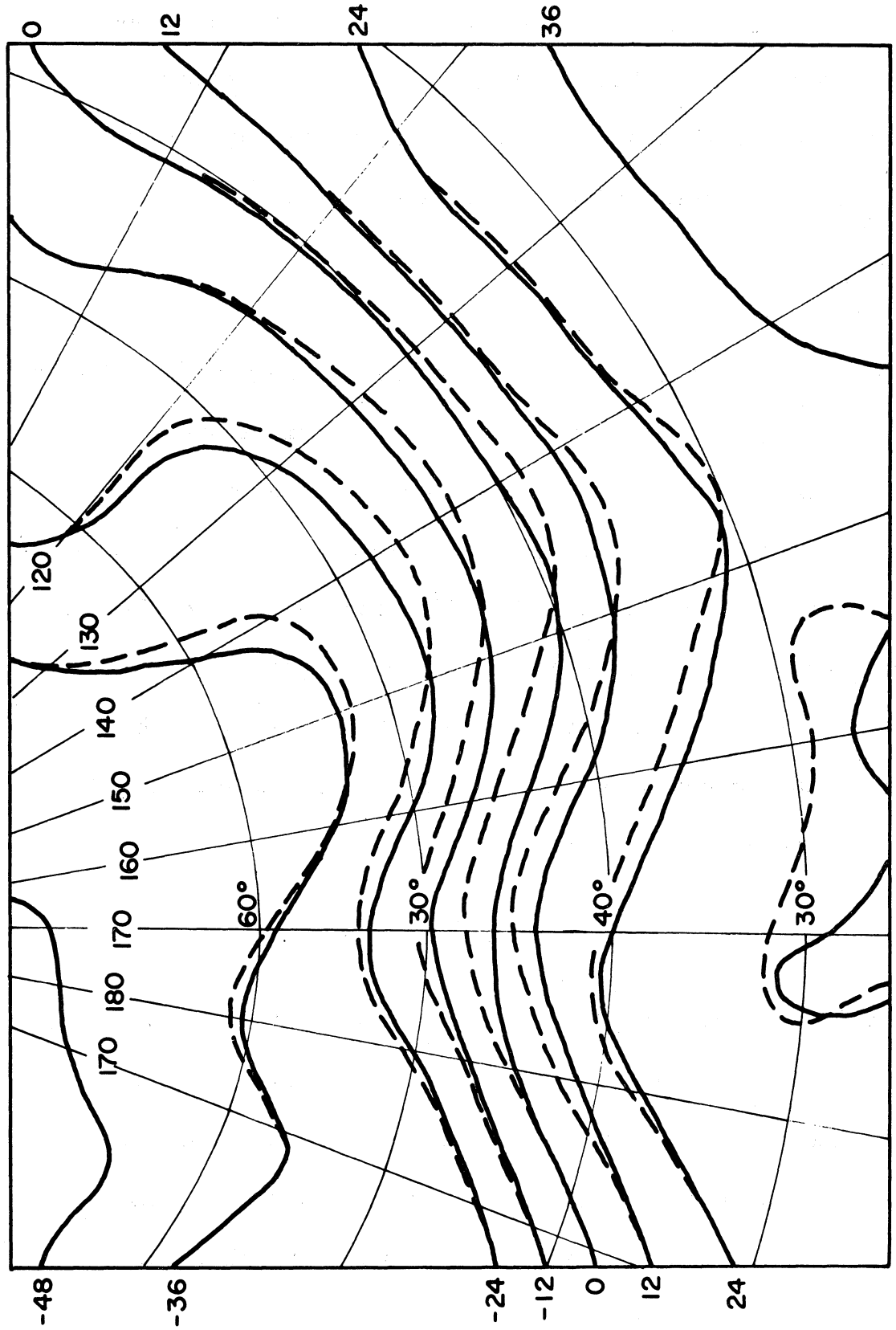

Figure 5.2. NMC numerical analysis (dashed lines) and SINAP relaxed stream field for case of 5 November 1963. Stream function $\hat{\psi}$ isopleths are D values labeled in tens of meters.

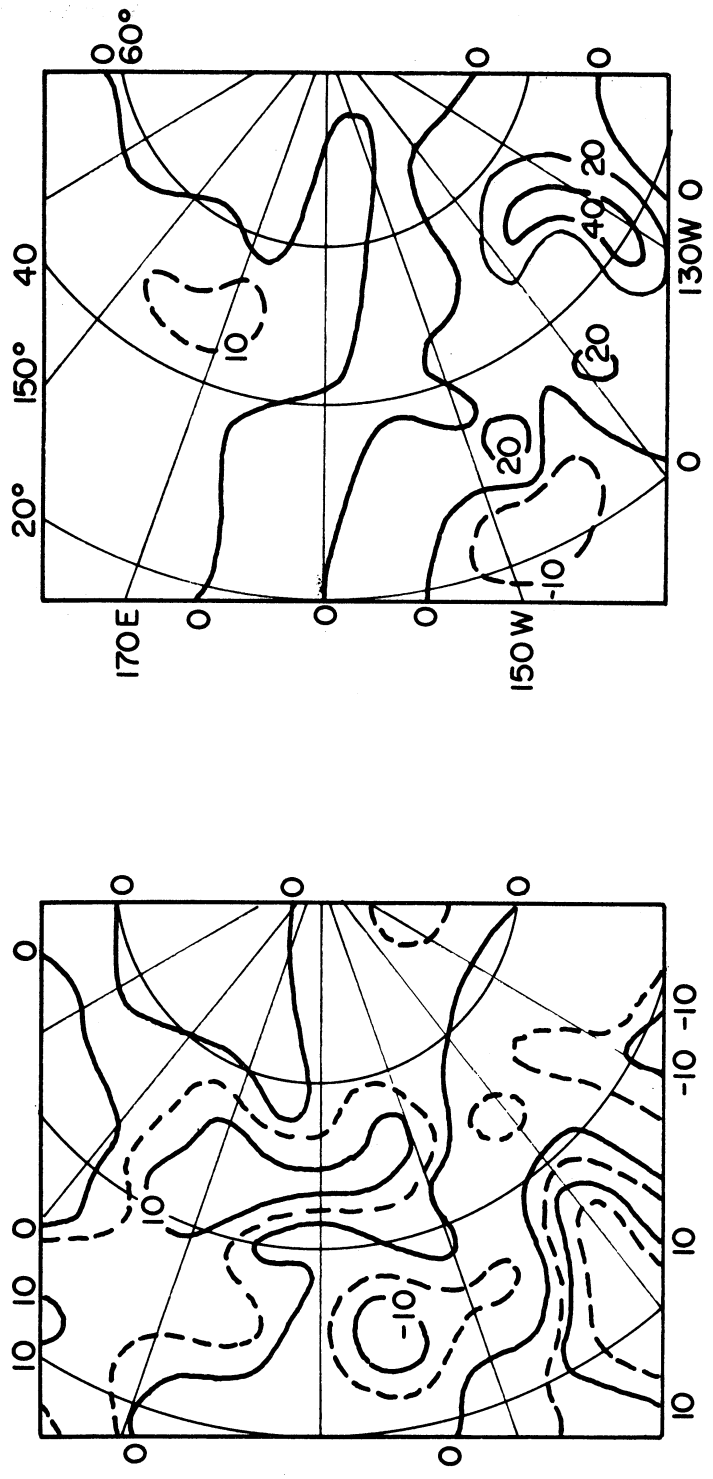

Figure 5.3. Left: NWP forecast minus observed for 1200GMT 6 November 1963. Isopleths are stream function $\hat{\psi}$ differences labeled in tens of meters. Right: Forecast improvement chart for SINAP reanalysis of 5 November case. Isopleths are stream function $\hat{\psi}$ improvements labeled in meters.

meters, it was not considered that the changes were distinguishable from chance.

	0	1	2	3	4	5	6
00Z 5 JNWP							
45°N	.64	.44/47	.05/214	.28/157	.61/112	.54/196	.88/109
30°N	2.21	.38/193	.50/82	.35/204	.29/85	.15/177	.39/23
JNWP FCST							
45°N	.66	.27/80	.26/335	.73/143	.52/133	.27/110	.71/169
30°N	2.17	.31/220	.75/331	.19/214	.37/88	.15/130	.19/331
12Z 6 JNWP							
45°N	.64	.36/50	.24/158	.60/149	.70/161	.11/81	.66/157
30°N	2.25	.48/171	.45/52	.17/214	.56/82	.25/254	.67/68
HINDCAST							
45°N	.59	.68/46	.34/165	.30/236	.75/150	.37/224	1.09/104
30°N	2.16	.53/177	.26/69	.33/229	.23/86	.22/286	.70/77
REFORECAST							
45°N	.57	.46/43	.30/125	.57/164	.63/167	.13/76	.62/157
30°N	2.20	.40/174	.58/42	.21/196	.56/97	.28/278	.62/62
JHB3 ANAL							
45°N	.65	.44/40	.13/182	.22/143	.58/120	.50/189	.81/109
30°N	2.21	.38/197	.52/86	.32/207	.28/90	.14/169	.38/205
JHB3 FCST							
45°N	.47	.18/166	.48/25	.49/175	.64/122	.20/126	.60/168
30°N	2.17	.32/222	.78/34	.21/222	.39/90	.13/127	.18/329
ZERO ABS VORT							
45°N	.97	.50/44	.09/132	.27/159	.62/110	.55/196	.87/108
30°N	1.96	.32/189	.57/80	.36/204	.30/88	.13/178	.38/23

TABLE 5.1

Amplitudes (Cm.*1E4) and Phases (deg.E) of Zonal Wavenumbers 0-12, 5 November 1963 Case.

	7	8	9	10	11	12
00Z 5 JNWP						
45°N	.33/209	.52/77	.15/356	.32/223	.12/311	.09/294
30°N	.26/129	.12/187	.09/312	.11/131	.11/74	.12/109
JNWP FCST						
45°N	.20/22	.46/199	.29/102	.14/147	.12/137	.15/119
30°N	.13/316	.10/165	.17/134	.08/144	.06/147	.15/149
12Z 6 JNWP						
45°N	.20/166	.32/211	.29/90	.70/64	.12/252	.15/76
30°N	.33/182	.23/214	.14/75	.10/36	.02/253	.11/102
HINDCAST						
45oN	.26/252	.51/63	.24/316	.02/221	.11/340	.03/40
30°N	.17/204	.10/156	.24/344	.09/183	.04/123	.07/79
REFORECAST						
45°N	.22/0	.32/197	.28/83	.07/47	.07/239	.11/86
30°N	.25/17	.20/207	.16/63	.06/354	.24/250	.13/100
JHB3 ANAL						
45°N	.34/198	.51/70	.10/352	.37/23	.14/295	.06/311
30°N	.27/129	.11/190	.08/308	.11/128	.10/74	.12/109
JHB3 FCST						
45°N	.24/354	.42/193	.35/95	.23/137	.17/163	.23/129
30°N	.13/319	.11/170	.18/130	.06/151	.08/153	.14/142
ZERO ABS VORT						
45°N	.32/207	.50/77	.16/359	.32/214	.13/312	.09/292
30°N	.24/131	.12/184	.08/312	.11/129	.10/71	.12/109

TABLE 5.1 (concluded)

Amplitudes (Cm.*1E4) and Phases (deg.E) of Zonal Wavenumbers 0-12, 5 November 1963 Case.

6. 26 JANUARY CASE

6.1 Synoptic Situation

The synoptic pattern of 26 January 1964 appeared promising for two reasons: firstly, the satellite photographs over the western Pacific revealed the presence of a large scale powerful system which was not apparent in the original JNWP analysis; secondly, verification statistics showed that the JNWP forecast for this period was outstandingly bad indicating fertile ground for improvement. Reproductions of the original analysis and the verification error chart are included as figures (6.1) and (6.2). It is apparent from the error chart that the maximum absolute error in the numerical forecast differed from the verification in excess of 500 stream meters; and in the area of the satellite coverage the difference exceeded 200 meters. This may be compared to the case of 5 November 1963, where the maximum absolute error was less than 200 meters.

The oustanding feature of the satellite photographs is the frontal cloud band which is clearly distinguishable in the second pass. This front was interpreted to be associated with a young cyclone nearing maturation or the occlusion stage. This was determined by the fact that the typical spiral nature of the mature cyclone is not in evidence, while the extreme clarity of the frontal band suggests the formative

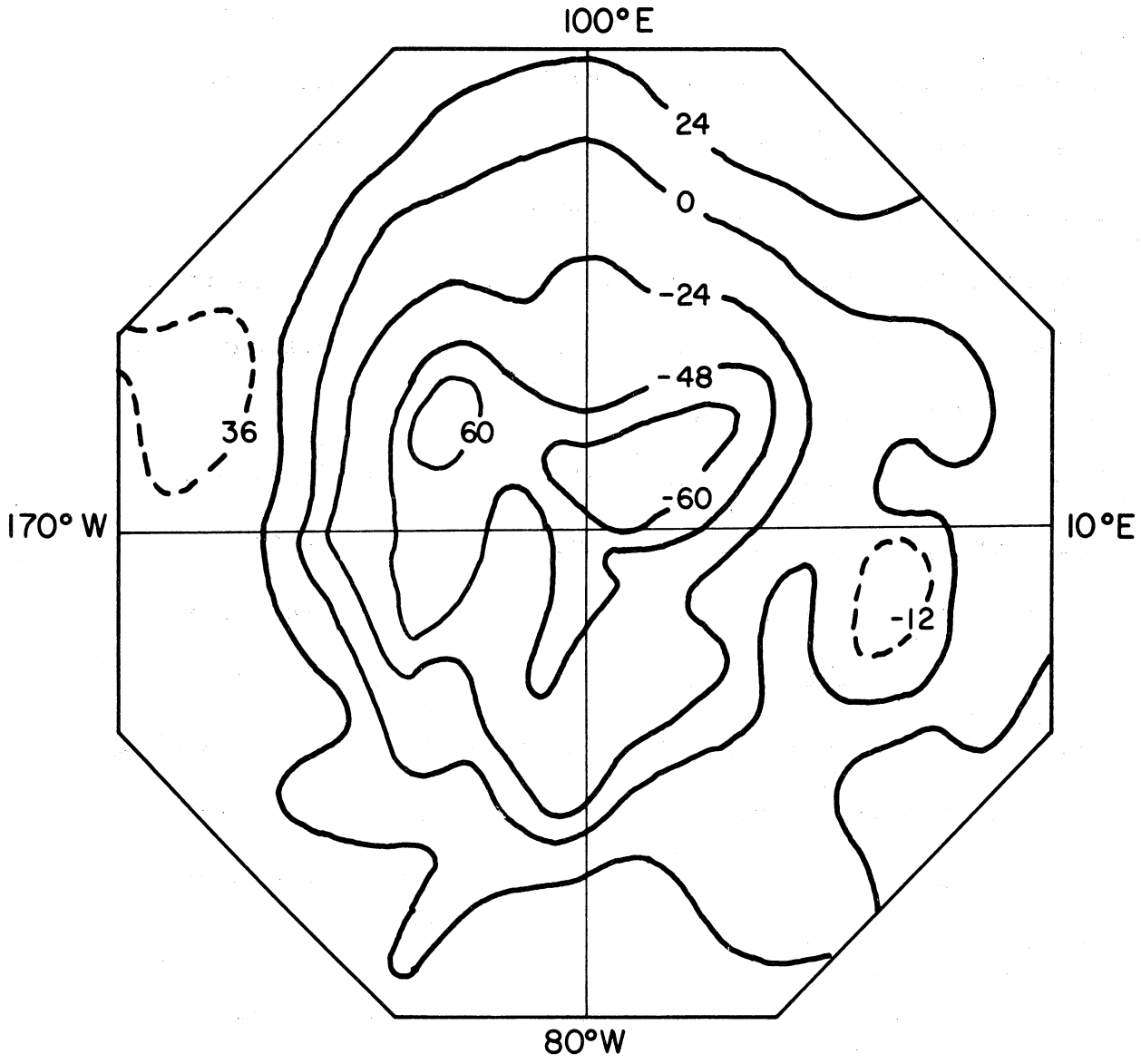

Figure 6.1. NMC numerical analysis for 0000GMT 26 January 1964. Stream function ψ isopleths are D values in tens of meters.

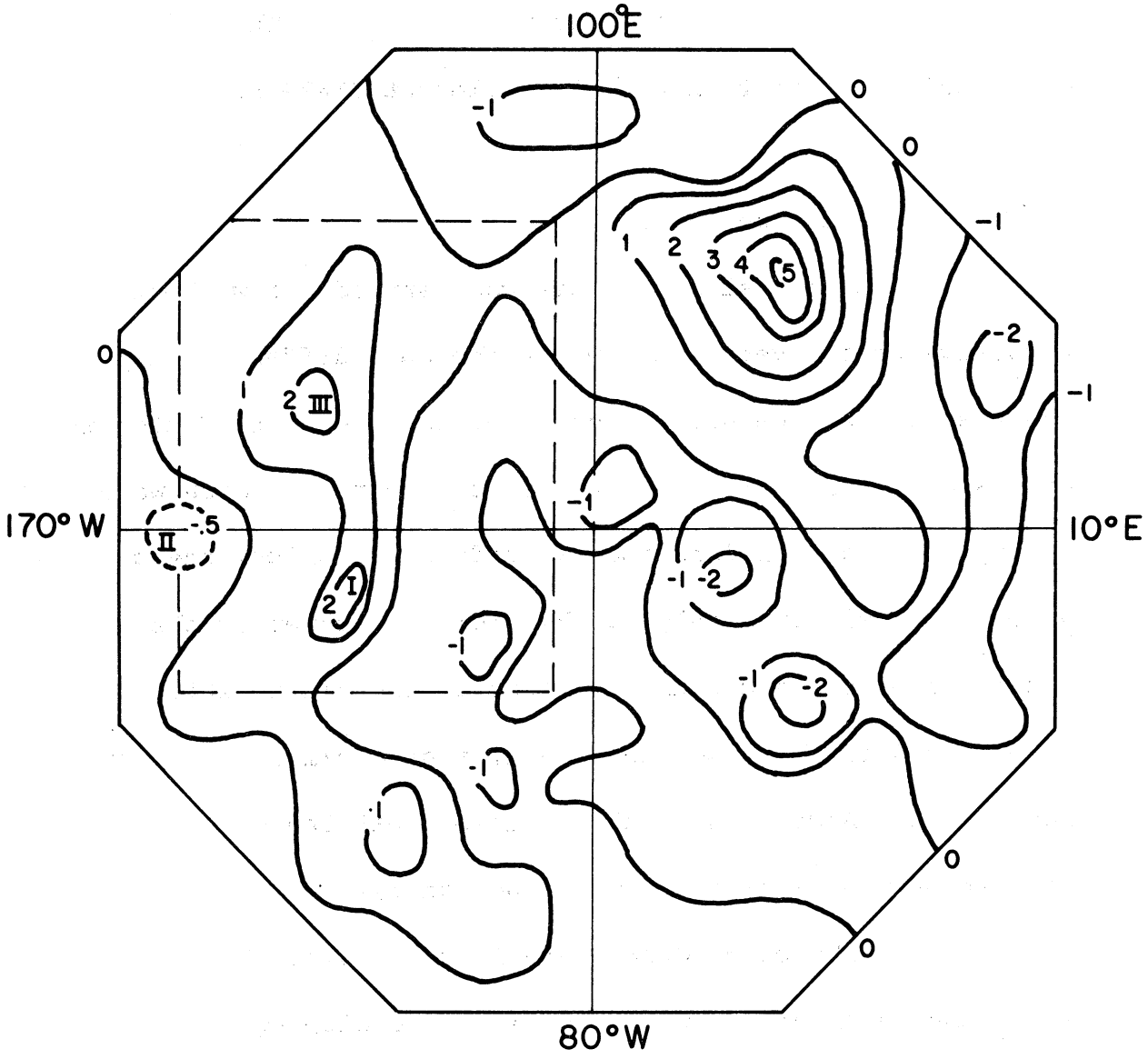

Figure 6.2. NMC forecast minus observed for 1200GMT 27 January 1964. Isopleths of stream function ψ difference are labeled in hundreds of meters. The dashed rectangle is the verification subset. Roman numerals identify error regions referred to in the text.

rather than the dissipative stage. The cyclone center was approximated to be 43°N, 174°E. A number of empirical rules concerning the flow aloft have been formulated by other researchers, and several of these were applied. They will be discussed in connection with the relevant SINAP reanalyses.

6.2 Streamline Reanalyses

I. The original reanalysis was carried out without knowledge of the verification nor the JNWP difference map. The reanalysis area was chosen to coincide with the satellite coverage (figure 6.3). Observations within this area were limited to Midway Island and two radiosonde ships, one of which was positioned only 500 km from the center of the satellite observed clouds. Because of the difficulties encountered in the 5 November case, a streamline reanalysis was chosen. According to the decision that the cyclone was not yet mature, a closed low was not analyzed on the 500 mb. surface (see Thompson, Cronin and Kerr (1964)). Further, since the major cloud areas visible in developing systems are almost certainly indicative of strong vertical velocities (rather than continuity), the trough line was accordingly positioned to the west of the major cloudy region. The actual magnitude of the displacement was necessarily

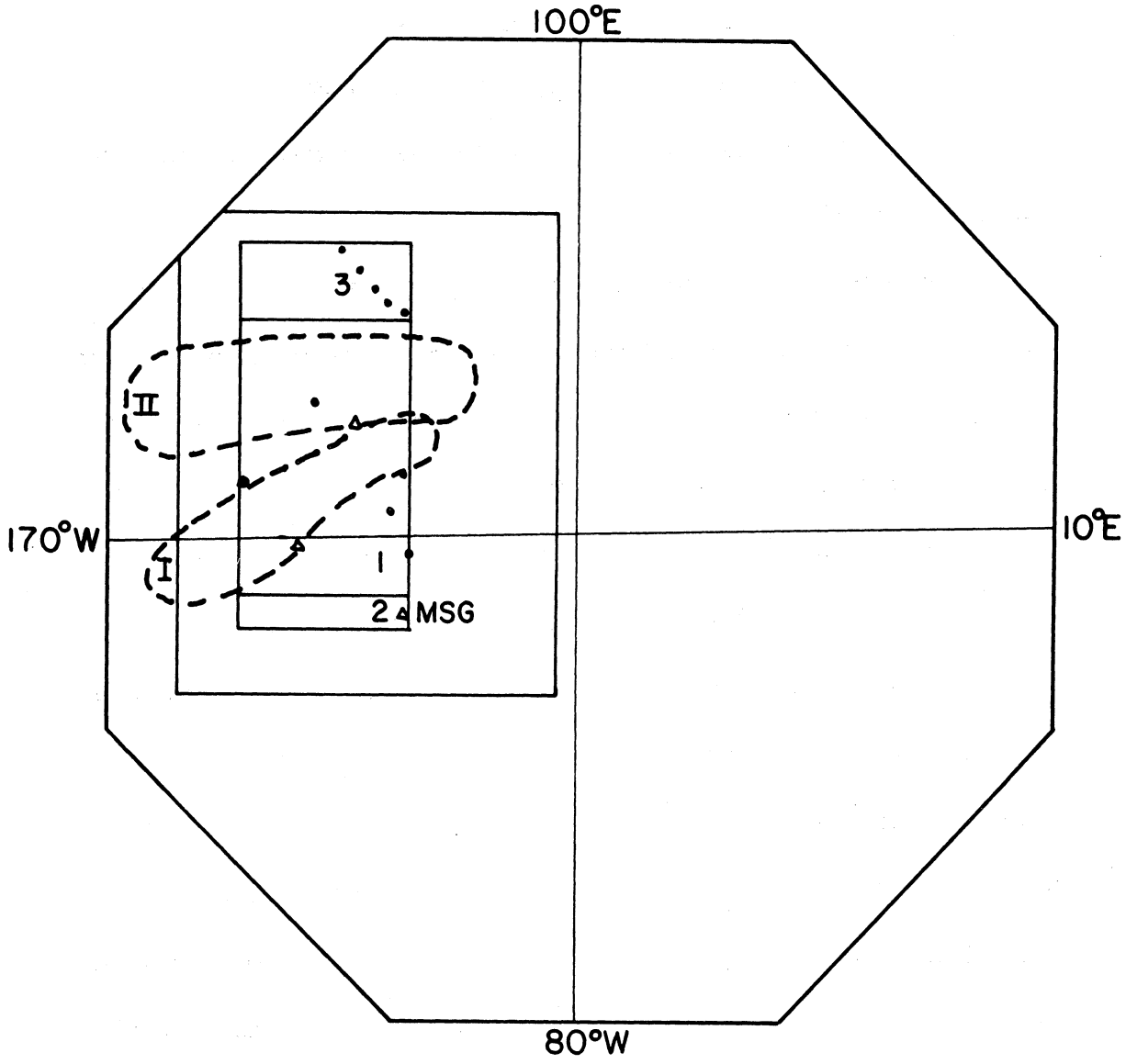

● Regular Radiosonde Stations

Δ Radiosonde only (No Winds)

MSG Missing data

Figure 6.3. Subareas used in 26 January stream function reanalyses and verification. Satellite coverage is indicated by the dashed curves. I is TIROS 7 orbit 3263 for 0342GMT; II is orbit 3264 for 0521GMT 26 January 1964. Rectangle 1 was included in reanalyses 1-6. Rectangle 2 was added for reanalysis 3. Rectangle 3 was added for reanalyses 4-6. The exterior rectangle is the verification subarea.

somewhat arbitrary, as no prior maps were available and thus no estimate of the speed of the system could be calculated. To account for the baroclinicity, and the time difference between satellite observation and analysis time, the trough line was established at 165°E.

On the basis of the slight changes resulting in the SINAP forecast for the 5 November case where changes in the reanalyzed streams were at maximum 86 meters, it was felt that more drastic modifications could be permitted. Accordingly the stream height in the trough area was decreased by a maximum of 178 meters. Further decrease was restricted by the observed data from the ships. To provide additional contrast with the original analysis and a steeper gradient on the leading edge of the trough, ridging to a maximum change of 324 meters was introduced downstream from the satellite coverage. Very modest ridging was also introduced upstream. The shaping of the trough, after the trough line was geographically positioned, was largely determined from the observed winds contained in the ship data, and the resulting scale of the system approximated wavenumber 12. Maximum changes in the vorticity introduced by the stream changes amounted to +305 meters.

II. With the identification of erroneous data from

the verification of the first reanalysis (section 6.4), a second reanalysis was made to measure stream curvature effect in a SINAP reanalysis, the streamlines in the reanalysis area were made as zonal as possible within the restrictions offered by continuity of the mean latitude of the zonal jet and the observed data within the area. This reanalysis was performed without consideration of the satellite data. The effect on the JNWP analysis was to fill the erroneous trough, slightly fill the central portion of the cyclone evidenced in the satellite photographs, and deepen the southern-central region of the reanalysis area. The changes nowhere exceeded 107 meters. The Laplacian calculated from the modified stream field also showed only moderate changes, nowhere exceeding 189 meters. The changes of the vorticity were almost exactly opposite to what is indicated by the satellite coverage, but as this reanalysis was intended to serve only as a standard of comparison, the reanalysis was not altered.

III. One reanalysis was made to incorporate empirical rules postulated by Thompson et.al. These investigators found that old polar fronts south of fresh polar outbreaks can frequently be distinguished in the Pacific by east-west bands south of 30°N, and this may reflect some regeneration of the old front. Though such a band is not clearly

distinguishable in the coverage of 26 January, there is slight indication of such a front in the first pass of the satellite. Because the secondary front was so close to the limit of the satellite coverage, the reanalysis area was extended two gridpoints to the east. Furthermore "cold migratory surface highs with westerly flow aloft appear as distinct clear areas. With more northwest to northerly flow aloft, there is a tendency for cellular clouds in the area." Since the cellular clouds are clearly represented in the satellite photographs, it was decided to enhance the ridging behind the cyclone in order to induce a more northerly flow. The reanalysis was constructed by graphical addition of two wave systems which were intended to represent the old polar front and the fresh outbreak associated with the strong frontal band in the satellite photographs. As a result, a rather broad trough was introduced into the reanalysis area. Relative to the first reanalysis, the trough line was moved east to approximately coincide with the center of the crescent-shaped cloud pattern. The maximum deepening was also displaced slightly south by the addition of the second system. Ridging ahead of the system was curtailed, while ridging to the rear was enhanced. Maximum deepening in the trough was 210 m., while maximum ridging behind the

system was 97 m. Maximum ridging downstream was reduced to 133 m. (largely due to the removal of the erroneous trough). The maximum positive relative vorticity change associated with the modified stream field was 276 m.

IV. A fourth reanalysis was constructed to emphasize ridging both up and downstream from the main cloudy area. Since the system in the first reanalysis was felt to be somewhat too baroclinic, the trough line was repositioned approximately three degrees to the east (168^{o}E). Troughing in the area of the cyclone was held to a minimum with stream modifications not exceeding -72 m. while maximum increases up and downstream were 226 and 231 m. respectively. Error charts for the first and third reanalyses proved difficult to correlate with modifications of the respective analyses. A major purpose of this reanalysis was consequently to elucidate the effects of the forecast of the upstream ridging (reanalysis three) and downstream ridging (reanalysis one). The primary effect on the vorticity field was to introduce broad areas of anticyclonic vorticity ahead and behind the cloudy region (-144 and -180 m) with a moderately small area of cyclonic vorticity increase in the area of the cyclone (+288 m.). The modified stream field is portrayed in figure (6.4).

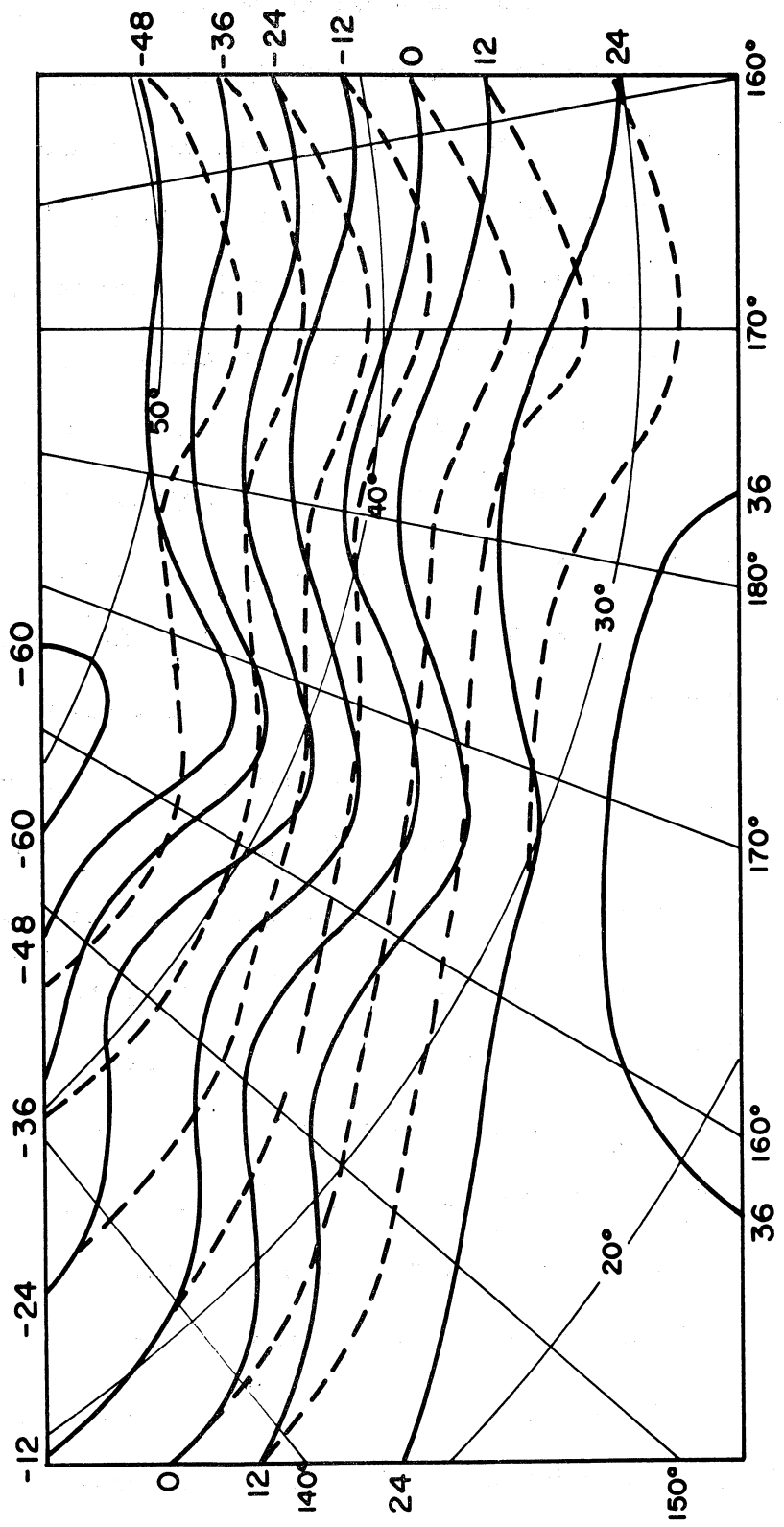

Figure 6.4. NMC numerical analysis (dashed lines) and SINAP reanalysis 4 (solid lines) for case of 26 January. Stream function ψ isopleths are D values labeled in tens of meters.

V. The fifth and sixth reanalyses were modifications of the fourth. It was felt at this time that the forecast could not in this particular case be significantly improved even by immoderate reanalyses. Consequently, attention was turned to the quantitative effect of alterations in the horizontal shear or the stream function gradient. In these three reanalyses, the curvature was held approximately fixed, within the constraints offered by continuity at the edges of the reanalyzed area. Intensity variations were not large, and so the three reanalyses test the sensitivity of the forecast to moderate changes in the shear.

In the fifth reanalysis, ridging both up and downstream from the cyclone was further enhanced to change maximum of 257 and 278 m. respectively. Depression in the trough region was not altered from reanalysis 4. Predictably, in view of the finite difference scheme employed in its computation, the general vorticity pattern was not significantly altered but the magnitudes were intensified. Maximum change values in the downstream ridge, the trough, and the upstream ridge were -180, 398, and -253 m. respectively.

VI. In the sixth reanalysis, the downstream flow was not significantly altered while the trough was deepened to a change maximum of -108 m. and the upstream ridge was

reduced to a change maximum of 178 m. The asymetric change in the stream function also changed the vorticity pattern such that the positive alterations in the trough area were considerably expanded. Maximum change magnitudes in the downstream ridge, the trough, and the upstream ridge were -234, 218, -278 m. respectively.

6.3 Vorticity Reanalyses

For completeness, two vorticity reanalyses were also made for the case of 26 January. The principal aim of the experiment was to achieve maximum simplicity in the reanalysis procedure. Consequently, the reanalysis region was reduced to a 9 x 6 gridpoint area. In both trials an area of very strong positive vorticity was introduced. The maximum changes were centered approximately 3^{o}WNW of the center of the crescent shaped cloud pattern as suggested in the Meteorological Satellite Laboratories "SINAP Procedures for 500-mb analysis modification." Negative vorticity modifications were introduced around the maximum, with a balancing region of negative vorticity in the approximate region of the upstream ridge. The magnitudes of the changes were made to conform approximately to those induced in stream function reanalyses 4-6. It should be noted that

changes of this size cause alterations in the stream function well beyond the limits of the reanalysis area. Consequently, changes which are not insignficiant (50 m.) do occur over relatively dense data areas in the U.S.S.R. However, the gradient of the change outside the reanalysis area is not large and so the dynamic effect on the forecast can be expected to be small. This assumption is certainly justified for the case of 26 January where the forecast error is so large. More importantly, large vorticity changes in a reanalysis necessarily violate neighboring observations in the reanalysis area. As remarked previously, radiosonde data was available within 500 km. of the center of the cloudy region, and this data could not be conserved when large vorticity changes were introduced.

I. In the first reanalysis the area of cyclonic vorticity change was chosen to be nine (3 x 3) gridpoints. The maximum change introduced was 300 m. The balancing region of anticyclonic vorticity was also nine gridpoints, but with a maximum intensity of only -120 m. Through an oversight the total relative vorticity in the reanalysis area was not conserved; however, the relaxed stream field changes were considered satisfactory for a forecast. A comparison of the stream function changes for this reanalysis and the second

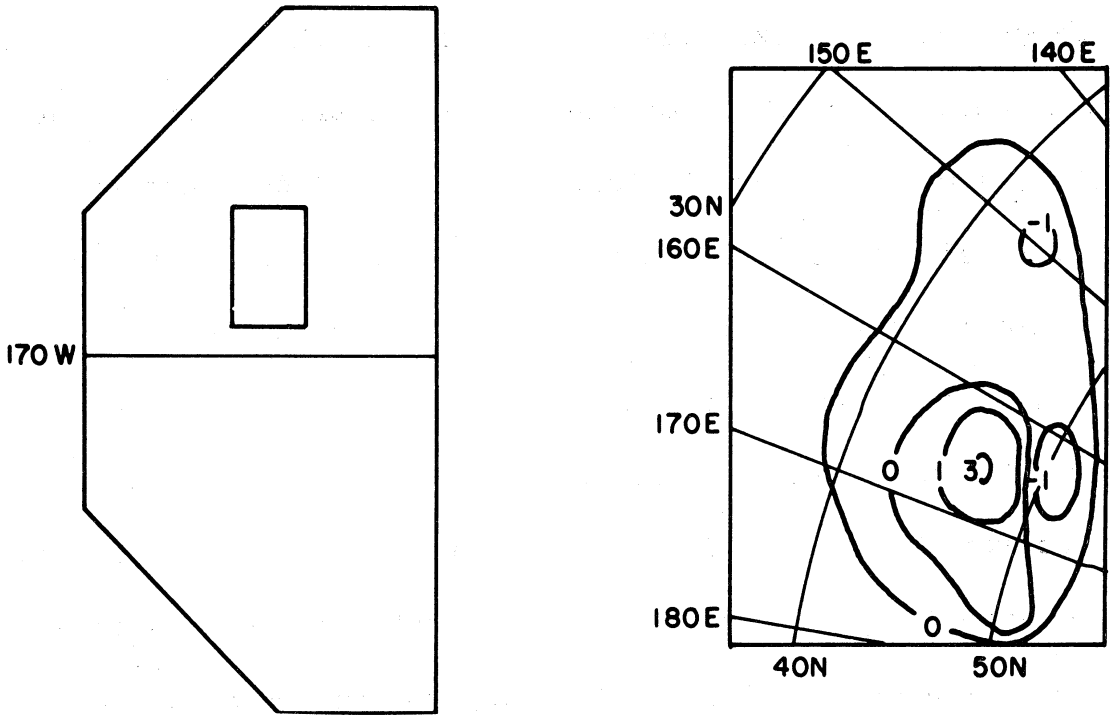

Figure 6.5. Above: Reanalysis area and Laplacian change field for vorticity reanalysis 1 for case of 26 January. Units are in hundreds of meters. Below: Relaxed stream field changes. Units are in tens of meters.

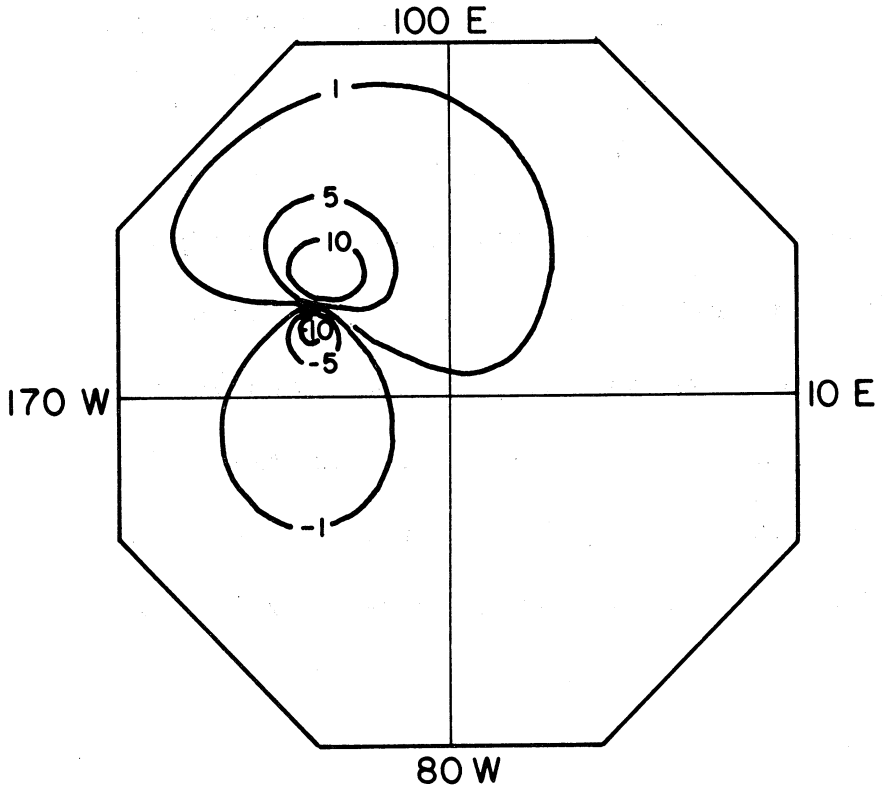

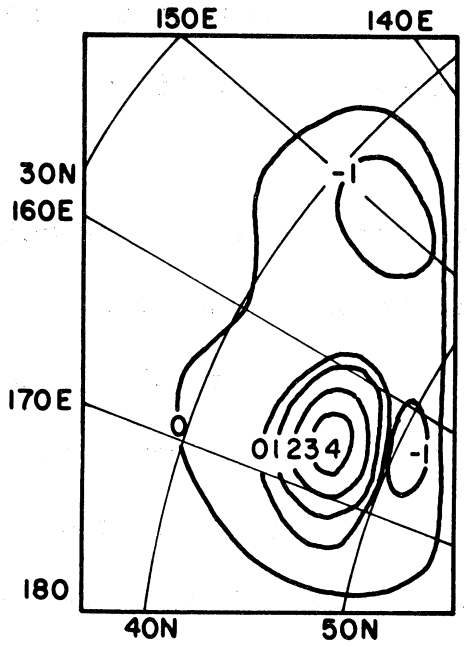

Figure 6.6. Laplacian change field and relaxed stream change field for vorticity reanalysis 2 for case of 26 January. Units as in fig. 6.5.

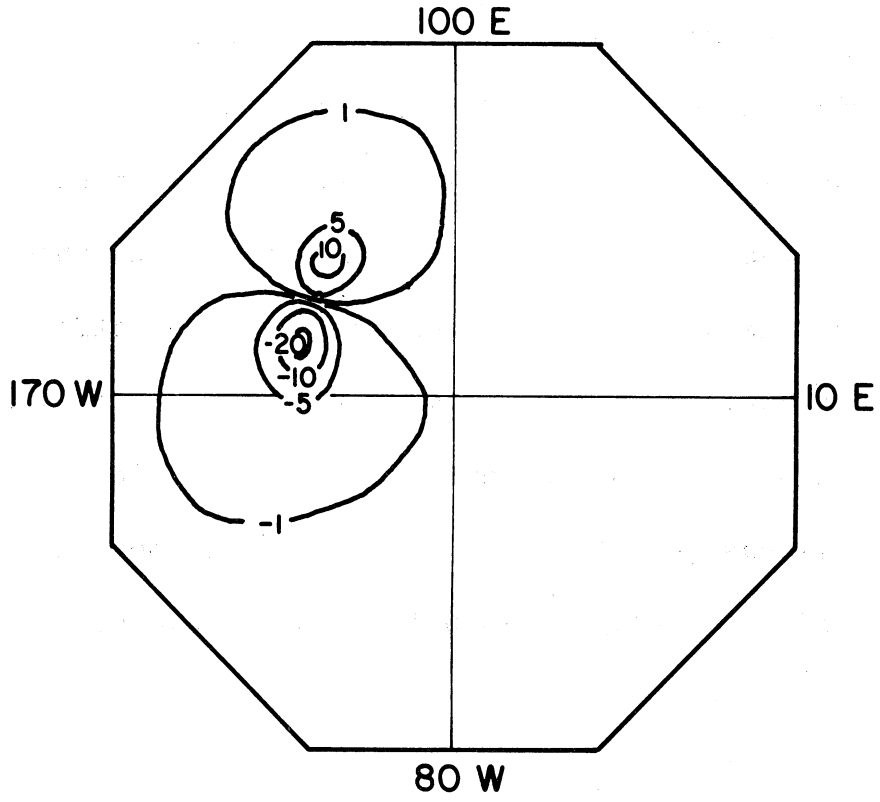

Laplacian reanalysis (which was more intense) shows the spreading effect when relative vorticity is not conserved (figures 6.5 and 6.6).

II. The pattern for the second Laplacian reanalysis was not altered, but the magnitude of the cyclonic maximum was increased to 400 m. Negative values surrounding the maximum of anticyclonic vorticity could not be increased without the introduction of negative absolute vorticities. This was avoided for reasons set forth in section 4.

6.4 Verification

A partial list of verification statistics is given in Table 6.1. It is apparent from these that the errors in the original JNWP forecast and all reanalysis forecasts are so large that the statistics have little meaning. In view of the original error, it would be unreasonable to expect significant improvement in the verification over the entire grid. The fact that none of the SINAP forecasts show any improvement is somewhat unsatisfactory. In an effort to investigate this a comprehensive point by point analysis of the differences and forecast improvement charts has been made. This has permitted some insight into the effects of the individual reanalyses as will be discussed below, but

CORRELATION COEFFICIENTS

Field	JNWP	SINAP 1	SINAP 3	SINAP 4	SINAP 5	SINAP 6	SINAP 7
Wind Grid	.49	.43	.46	.46	.44	.45	.48
Wind Sub	.49	.40	.34	.41	.33	.37	.38
Stream Grid	.39	.32	.34	.33	.36	.30	.38
Stream Sub	.59	.38	.38	.36	.47	.28	.60
Lap Grid	.65	.53	.55	.52	.53	.55	.54
Lap Sub	.67	.40	.39	.32	.39	.46	.42

R.M.S. ERROR

Wind Grid	12	14	13	14	14	14	12
Wind Sub	10	17	13	16	15	16	11
Stream Grid	9481	10394	9934	10040	9954	10364	9387
Stream Sub	7913	11158	9528	10052	9386	11538	6780
Lap Grid	3878	4748	4472	4737	4784	4649	4157
Lap Sub	4105	6826	6036	6804	6912	6284	5111

TABLE 6.1

Verification Statistics for SINAP Stream Function (1,3-6)
and
Laplacian (7) Reanalyses

has not suggested any manner of significantly improving the forecast.

Several points should be noted concerning the verification stream field and the difference chart computed from the JNWP forecast and verification fields. The verification streamlines over the Pacific exhibit a wave pattern approximating wavenumber nine. The JNWP forecast streamlines on the other hand show little wave pattern whatever, and consequently the difference map is composed of fairly well ordered error maxima (figure 6.2). These maxima, moreover, are rather well correlated with the Pacific observing stations. This is felt to be quite meaningful in view of the arguments presented in section 3.1.

The scale chosen for the SINAP reanalyses on the basis of the satellite data was wavenumber twelve, which turns out to be a fair approximation for the observed discrepancies. However, in no instance did a SINAP forecast approximate the wave pattern of the verification. The two entities therefore appear to be unrelated.

Completion of the first SINAP forecast revealed that both it and the JNWP forecast mistreated a blocking pattern in the eastern Pacific near the west coast of North America. In both forecasts the block was to some degree broken, while

the verification analysis showed it to have intensified. In view of the dominant role played by a blocking pattern in the general circulation, much of the error in the numerical forecast may be attributable to this feature. An attempt was made to isolate the cause for the breaking of the block but although this uncovered an erroneous observation in the central Pacific (corroborated by the Satellite Laboratories) the removal of a trough induced by the faulty data did not affect the behavior of the block in the forecast. Similarly, none of the SINAP forecasts altered the original behavior as the satellite coverage was too far removed.

The major error regions in the verification subareas are labeled in figure (6.2). They will be referred to by number in the following discussion. As expanded below, only error I appears to be significantly correlated with the satellite observed weather system. Errors II and III, while influenced in magnitude by the reanalyses could not be changed in pattern. The verification of each error region is discussed separately below in terms of the stream function and Laplacian reanalyses.

In most of the stream function reanalyses, error I is the region into which the satellite observed system is moved by the forecast. It represents a region where the JNWP forecast exhibits too little troughing. This error was, however,

intensified in all the stream function reanalyses except the third. On this basis it is tempting to ascribe the discrepancy to ridging introduced downstream from the satellite observed clouds. This is clearly the case with the first reanalysis as the development followed throughout the forecast period shows amplficiation of the downstream ridge with the low center consequently steered too far to the north. However, in reanalyses 4, 5 and 6, there is also an effect from the ridging introduced upstream. In these trials the downstream ridging did not develop significantly, and the additional upstream ridging was advected into the error region. The end result on the difference maps is the same in all cases, but for intricately different reasons. In all cases the major failure results from insufficient troughing in the reanalyses, as ridging effects were emphasized.

For reanalyses 4, 5 and 6, which were carried out to investigate the effects of slight changes in the shear, slight modifications had significant influence on the error field (figure 6.7). However, it proved to be impossible to correlate the analysis and forecast changes because of the complex interdependence of the two ridges. For example, the error was extremely similar in reanalyses 4 and 6 although in the latter analysis the upstream ridge had been intensified

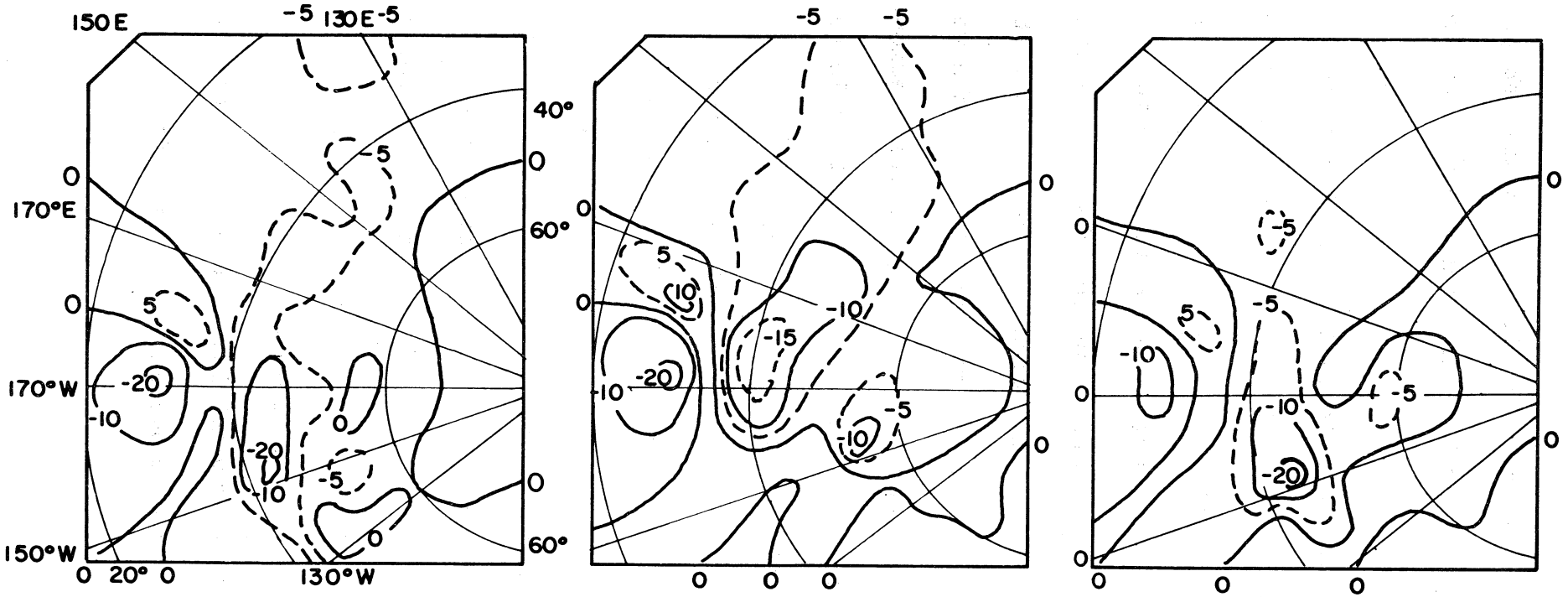

Figure 6.7. Subarea forecast improvement charts for (left to right) SINAP stream function reanalyses 4, 5 and 6 for case of 26 January. Stream function difference isopleths are labeled in tens of meters.

while the downstream ridge was weakened. Inexplicably, the forecast of reanalysis 5 was significantly different from either.

It is evident from the Laplacian reanalyses' forecasts that the influences on error II were largely derived from the positioning and intensity of the upstream ridge which governed the extent to which the trough penetrated southward in the forecasts. It is consequently apparent that if the satellite observed system is to have any effect on this error, it will be in the nature of additional troughing. Since the verification chart requires additional ridging in this region, it is highly doubtful that the discrepancy is attributable to the system observed in the satellite photographs.

The effect on error II of the upstream ridging was most clearly demonstrated in reanalyses 4, 5, and 6. In all cases erroneous troughing was forecast in this region. The change was especially pronounced (200 m.) for reanalyses 4 and 5 where the anticyclonic gradient introduced upstream from the trough proved to be unstable and caused explosive deepening of the system. For reanalysis 6, with the ridge modified, the effect was less intense (100 m.).

Error II was also intensified in the second reanalysis which was an attempt to remove all curvature effects. An

(This page is blank.)

analysis of the six hourly forecasts showed that this was caused by lowering the mean height just west of the erroneous trough. This particular adjustment was unconnected with the satellite observed cloud patterns suggesting that the error itself is unconnected with the observed system.

Error III like Error I represents an area where the forecast failed to produce a trough. This error was neither significantly nor systematically altered in the stream function reanalyses' forecasts.

The vorticity reanalyses proved to be slightly more encouraging than the stream function reanalyses, even though the initial stream field was extremely noisy. In both trials error I was slightly improved (figure 6.8). This may be attributed in part to the removal of the downstream ridge but is largely a consequence of the repositioning of the upstream ridge to the northwest and the broadening of the trough in the cloudy region. The figure also reveals the introduction of a fictitious low center to the north of error I. This represents a direct advection of the original low center in the reanalysis and indicates that the original center was both slightly malpositioned and too intense.

Although the change of the position of maximum ridging upstream from the cloudy area was only 5^{o}, this was sufficient

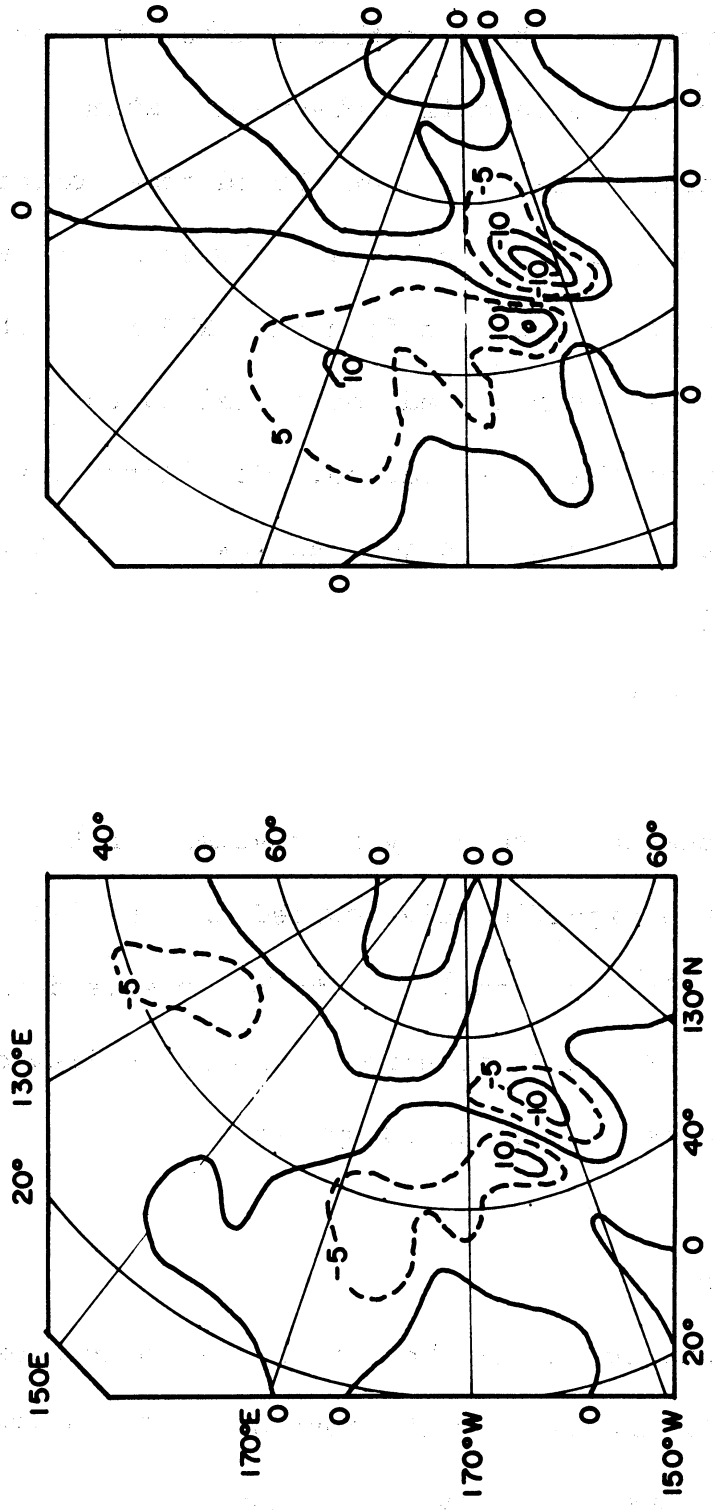

Figure 6.8. Subarea forecast improvement charts for (left to right) SINAP vorticity reanalyses 1 and 2 for case of 26 January. Units as in fig. 6.7.

to almost entirely eliminate influence on error II. This gives further support to the hypothesis that that error is not associated with the satellite observed system.

Both Laplacian reanalyses contributed some corrective troughing in error III. In both cases, however, the area of maximum error is undisturbed from the JNWP forecast since the SINAP forecasts, as measured above, failed to produce the wave pattern of the verification. To a large extent this improvement is the result of a general lowering of the height of the stream field, and analysis of the six hourly forecasts shows that this lowering is retained from the original field. This is consistent with the failure of the stream function reanalyses' forecasts to show any improvement in this region, as they in no case significantly lowered the initial heights. This improvement is thus considered to be to some degree fortuitous, and error III, as error II is not believed to be related to the satellite observed system.

6.5 Conclusions

In some instances it has been possible to draw cause and effect relationships from the forecasts of the SINAP reanalyses. In general, however, the internal mechanics of the forecast are too complex to permit formulation of any

specific rules. The separate effects of shear and curvature on the forecast could not be distinguished. As a rule of thumb the magnitude of the forecast changes approximates the magnitude of the initial changes, but the direction of propagation is extremely sensitive to rather small differences.

Analysis of the verification maps for this case points out the importance of the geographic positioning of a satellite observed weather system. In particular, the Laplacian reanalyses demonstrated that a shift of a few gridpoints in the upstream ridge influenced an entire region (error II) of the forecast. Although this problem was probably emphasized in this work by the immoderate size of the analysis changes, it is hardly doubtful that it would exist in all cases.

LAT.	20	30	40	45	50	60	70	80
00Z 26 Jan	1.68	.72	1.30	2.33	3.15	4.18	4.96	5.99
JNWP	1.30/219	1.61/236	1.32/276	1.22/299	1.25/366	1.13/330	.90/262	1.42/259
12Z 27 Jan	2.34	.56	1.42	2.54	3.38	4.30	4.86	5.99
JNWP	.77/187	1.48/227	1.44/294	1.81/322	1.70/324	.52/327	.29/95	.61/174
JNWP	2.10	1.11	1.00	2.28	3.41	4.64	5.06	6.06
FCST	1.26/184	1.28/199	.57/301	1.08/332	1.33/333	.59/334	.43/224	1.01/259
CMH1	2.10	1.09	.76	2.09	3.36	4.60	5.04	6.01
FCST	1.22/182	1.18/194	.51/254	.72/322	1.14/337	.60/329	.56/225	1.05/257
CMH2	2.11	1.09	.94	2.21	3.37	4.63	5.05	6.04
FCST	1.25/184	1.20/198	.54/292	.96/327	1.23/333	.58/333	.54/225	1.02/259
CMH3	2.11	1.10	.70	2.04	3.37	4.62	5.04	6.04
FCST	1.20/184	1.12/192	.54/251	.72/320	1.10/339	.57/339	.52/223	1.01/259
CMH5	2.11	1.11	.71	2.05	3.33	4.59	5.02	6.04
FCST	1.17/179	1.10/191	.37/245	.68/332	1.15/341	.55/338	.52/221	1.01/259
CMH6	2.16	1.16	.93	2.23	3.35	4.55	4.99	6.04
FCST	1.26/180	1.17/194	.51/316	1.10/344	1.32/342	.51/349	.43/216	.95/264
CMH6	2.34	.78	1.31	2.42	3.28	4.13	4.91	5.95
ANAL	1.12/195	1.53/231	1.07/284	1.33/335	1.53/349	1.07/336	.82/260	1.38/258
CMH7	2.11	1.08	.98	2.36	3.52	4.66	5.10	6.13
FCST	1.24/184	1.17/201	.64/306	1.27/339	1.53/341	.62/345	.44/227	.97/265
CMH7	2.31	.71	1.44	2.59	3.42	4.23	5.01	6.04
ANAL	1.08/196	1.50/236	1.20/292	1.59/335	1.72/347	1.18/336	.85/265	1.39/260

TABLE 6.2

Amplitudes and Phases of Zonal Wavenumbers 0 and 1,
26 January 1964 Case

LAT.	20	30	40	45	50	60	70	80
CMH8	2.13	1.12	.81	2.12	3.40	4.61	5.03	6.04
FCST	1.25/181	1.18/194	.43/268	.81/326	1.25/339	.59/336	.54/223	1.03/258
HINDCAST	2.42	.78	1.19	2.12	3.05	4.42	5.06	5.96
OMEGA=1.4	1.15/175	1.76/206	1.36/270	1.91/306	1.84/321	1.20/341	1.14/130	.46/141
REFORECAST	2.32	.99	.97	1.94	2.99	4.69	5.28	5.99
	1.34/162	1.74/184	.78/267	1.21/317	1.24/326	.26/177	1.22/138	.67/103
HINDCAST								
OMEGA=1.70	2.31	.66	1.61	2.57	3.32	4.09	5.02	5.95
AND 1.30	.45/198	1.31/251	1.68/313	1.68/329	1.56/339	1.22/344	1.37/290	.73/168
1/2 HOUR	2.30	.67	1.60	2.56	3.32	4.08	5.01	5.94
HINDCAST	.44/199	1.28/251	1.68/314	1.67/329	1.55/339	1.22/344	.14/290	.71/168
1/2 HOUR	2.25	.69	1.28	2.42	3.30	4.30	5.01	5.98
REFORECAST	.61/188	1.10/226	1.34/307	1.79/328	1.63/329	.53/322	.29/153	.58/188

TABLE 6.2 (concluded)

Amplitudes and Phases of Zonal Wavenumbers 0 and 1,
26 January 1964 Case

7. CONCLUSION

As a result of this investigation is is believed that SINAP procedure could not significantly alter the numerical forecasts in the cases studied. It is felt that for the case of 5 November the scale of the satellite observed weather system is too small to be effective whereas for the case of 26 January the initial state is too poorly specified on an hemispheric scale to be improved even by the proper interpretation of a moderately large system in the satellite photographs.

The greatest difficulty in the SINAP procedure remains the proper interpretation of the satellite observed cloud forms. The various trials with the case of 26 January point out that some improvement could be achieved in a limited region, but that this requires a very specific analysis of the system evident in the cloud photographs, particularly with regard to geographical position.

Verification of the SINAP procedure is obfuscated both by the scant data in the region of verification and by the complexity introduced by the numerical forecast. Under these handicaps it was found to be impossible to draw quantitative conclusions. In particular, it was not possible to distinguish in the forecast the individual effects of alterations in the shear and curvature. The complexity of the dynamic interaction

precluded their separate recognition although the combined effect is to preserve the magnitude of original alterations in the analysis.

The investigators found no inherent advantage to choosing a stream function rather than a vorticity reanalysis. From an operational standpoint, the difficulty in restricting the relaxed stream field changes is compensated by the ease of avoiding negative absolute vorticities and by the reduction of the area which must be reanalyzed. Delineation of their relative merits would require a more selective verification procedure than that utilized in this work.

Hindcast-reforecast procedures gave disappointing results due to the large truncation and other numerical problems found, but point to the conclusion that substantial baroclinic effects and errors not remediable by satellite data are present. Discrepancies in the balance equation are unexplained.

Changes in the forecast for different zonal wavenumbers are comparable in magnitude to changes in the analysis: differences in the zonal mean profile observed and forecast or hindcast are prominent.

8. SUGGESTIONS FOR FUTURE WORK

8.1 The Analysis Problem

The SINAP procedure was introduced to supplement observations over sparse data areas. Through the use of a numerical forecast, the resulting analysis may in principle be validated in a dense data area. However, in attempting to utilize the satellite photographs for reanalysis with forecast verification, this project has compounded the difficulties of weather system recognition with the purely mechanical problems of numerical prediction. Further, in practice the verification has also taken place over data sparse areas, and itself is thus suspect. It is felt that the chances for success in such a venture are rather limited.

The results of this project suggest that the proper interpretation of the cloud photographs remain the primary problem, and there is every indication that the analysis problem must be more fully investigated before adding the additional complexities of the numerical forecast. It is thus suggested that alhtough the prime purpose of a SINAP reanalysis is to supplement observations in a data sparse area, analysis techniques cannot be perfected over such areas, as they cannot be directly verified. Only when an analysis technique has been developed and tested over an area of fairly good conventional coverage can it be applied in data sparse areas. At this time verification

through forecast would be more feasible, especially as expanding satellite coverage might permit modification of the verification as well as the initial field.

Several factors which were not considered in the present project might be incorporated into such an analysis study. Following is a partial list.

8.2 Continuity and Winds

The isolated photographic swaths used in our studies did not allow any determination of wind speeds or directions from the displacements of identifiable features. Current coverage should allow the use of this method.

8.3 Thermal Radiation Data

Despite possible data processing problems, the use of thermal radiation data would substantially assist in guessing the height and type of stratiform clouds, and deducing the motion field.

8.4 Gandin's Method of Omitted Stations

In his comprehensive book on automatic analysis, Gandin (1963) omits some stations from a network in order to have comparison data for his analysis. This method would provide

a direct test of the ability of satellite data to improve the thermohydrodynamic analysis if used over the dense data areas of Europe and North America.

APPENDIX A

Successive Point Over-Relaxation

The theory of Accelerated Liebmann or Point Successive Over-Relaxation used in the NMC routine WPA13 is treated in many texts, e.g., J. Todd (1962), L. Fox (1962), D. K. Fadeev and V. N. Fadeeva (1963). The authors have not, however, found a discussion of the combined jury-marching method used in most forecast models. The constant omega (COEF) of 1.40B2 used in WPA13 is close to the overall optimum value (least number of scans) found by L. Norton (U.S.W.B; Fort Worth) in unpublished work on a 14*23 point 36 hour barotropic forecast during U.S.W.B. Refresher Courses at the University of Michigan in 1965.

Re-examination of Norton's results showed, however, that the best values for 14*23 are about 1.70 at the initial step and 1.30 at all subsequent steps. Further, a trial of Aitken extrapolation (Fox, p. 287) was found to require the assumption that the error vector at all steps after the initial time was dominated by one or more eigenvectors corresponding to eigenvalues much smaller than the spectral radius of the matrix. Under these circumstances Aitken extrapolation is of little value.

It may be shown (Dr. C. Young, private communication) that the theoretical optimum omega (for a minimum spectral radius of the relaxation matrix) is near 1.70, which coincides with the least number of scans only on the assumption that the error vector is reduced to a multiple of the special eigenvector (corresponding to the absolutely largest eigenvalue or spectral radius) before the convergence criterion is met.

In practical forecast procedures this requirements is met only at the initial step, when a first guess of zero is used for the tendency field: the error vector at convergence is then dominated by an eigenvector approximating to a hemispheric dome. At subsequent steps the tendency field from the previous time step is used as a guess, and the error vector at convergence is dominated by short wave motions represented by eigenvectors corresponding to eigenvalues far from the spectral radius; since there are many such eigenvalues, the problem of least-scan omega becomes statistical and in practice one can do no better than make omega a pre-determined function of time.

For a single jury problem such as a Laplacian reanalysis 1.70 would probably be best, but we have not tested this except of a 14*23 model.

Consider an arbitrary relaxation matrix A of order n, having eigenvalues $\lambda_1, \lambda_2, \ldots \lambda_n$ and corresponding eigenvectors $U_1, U_2, \ldots U_n$; and let the eigenvalues be ordered so that

$$|\lambda_1| > |\lambda_2| > \ldots > |\lambda_n|$$

In the iterative solution of the equation

$$Ax = b$$

let the kth approximation to the correct answer x be called x_k, and let the error vector

$$e_k = x - x_k.$$

Then (Fadeev and Fadeeva, Chapter V)

$$e_{k+1} = C_{1,k+1}U_1 + C_{2,k+1}U_2 + \ldots + C_{n,k+1}U_n$$

$$= \lambda_1 C_{1,k}U_1 + \lambda_2 C_{2,k}U_2 + \ldots + \lambda_n C_{n,k}U_n$$

on the assumption that the expansion can be made.

Then the error change vector

$$x_{k+1} - x_k = e_k - e_{k+1}$$

$$= (1 - \lambda_1)C_{1,k}U_1 + \ldots + (1 - \lambda_n)C_{n,k}U_n$$

$$= (1-\lambda_1)\lambda_1^k C_{1,o}U_1 + \ldots + (1-\lambda_n)\lambda_n^k C_{n,o}U_n.$$

It is usual to use the absolutely largest element (maximum modulus norm) of the error change vector as a convergence criterion. Evidently the problem of minimizing the number of scans in a jury problem can be reduced to the

problem of minimizing the spectral radius (absolutely largest eigenvalue) only if the special eigenvector comes to dominate the error vector at convergence; this is not so in jury-marching problems.

For any given eigenvector one may define an amplification factor by

$$a_m = C_{m,k+1} \; C_{m,k}$$

which for the accelerated Liebmann process leads to

$$a_m = \lambda_m \qquad m = 1, 2 \ldots n.$$

For an Aitken extrapolation by the formula

$$x_{k+2} = (x_{k+1} - cx_k) \; (1 - c)$$

where C is some arbitrarily assigned constant, the amplification factor for the mth eigenvector is

$$a_m = \lambda_m \; (L - C) - C.$$

Since the best value of C for a 14*23 model was found to be between 0 and 0.25, it is clear that after the initial time step the error vector is dominated by components corresponding to eigenvalues less than 0.1.

Figure A.1 shows the amplification factor as a function of λ for various values of C.

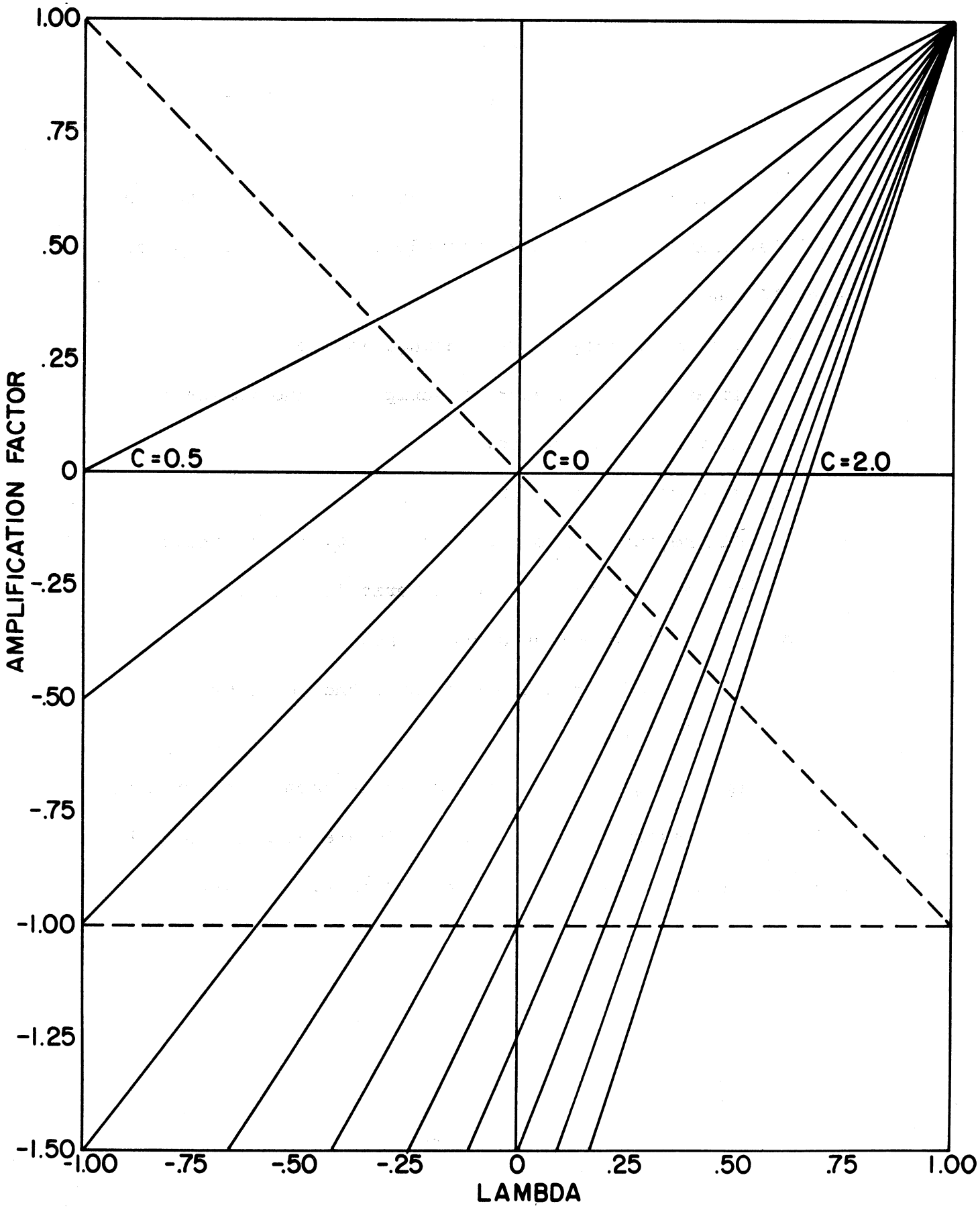

Figure A.1. Amplification factor against eigenvalue for different values of c in Aitken extrapolation.

APPENDIX B

Diagnostics for the NMC Barotropic Model

The following parameters are currently saved on tape A4 and later printed in I,J and latitude-longitude coordinates by a MAD-UMAP program:

1. The absolutely largest change in the WPA13 relaxation, its linear subscript and the forecast hour, at convergence.
2. #1 upon no convergence.
3. All negative absolute vorticities, their linear subscripts, and the local Coriolis parameter.
4. All on-line comments from WPK03.
5. In case of a fatal error exit, the whole of core in four blocks.

A tamper program allows a new master tape to be written with 28 secs. execution time. SPRA 1's are changed to SPRA 4 to suit the on-line printer belts used here.

APPENDIX C

Mosaics of TIROS Photographs, 26 January 1964

Following are the TIROS VII photographs used in reanalysis of the 26 January case.

DTG: 0342 Z

JAN 26 1964

ORBIT: 3268/3263

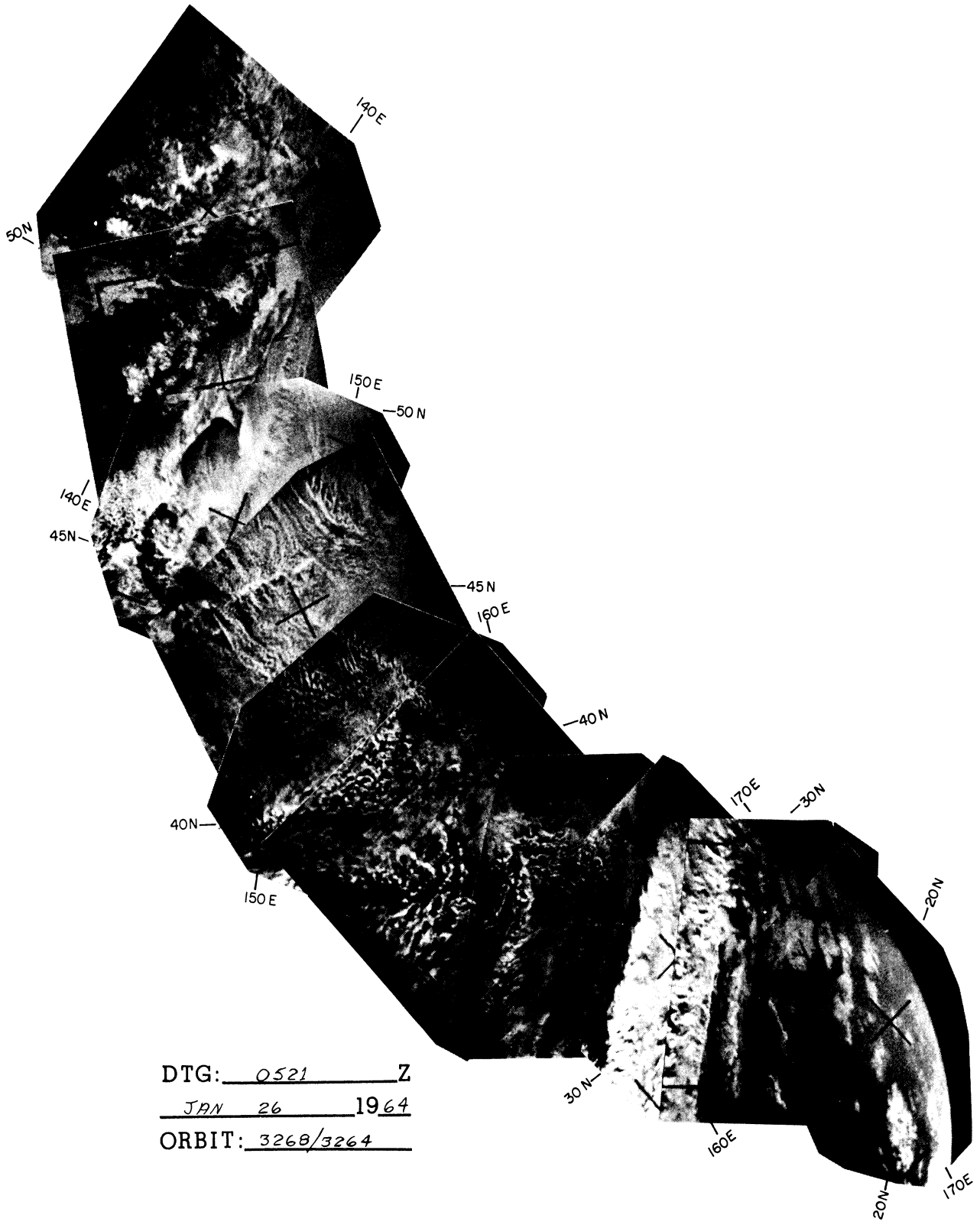

DTG: 0521 Z
JAN 26 1964
ORBIT: 3268/3264

BIBLIOGRAPHY

Fadeev, D. L. and V. N. Fadeeva, 1963: Computational Methods of Linear Algebra. W. H. Freeman and Co.

Fox, L., 1962: Numerical Solution of Ordinary and Partial Differential Equations. Pergamon Press.

Gandin, L. S., 1963: Obektivnii Analiz Meteorologicheskikh Polei. Gidrometeoizdat, Leningrad, Library of Congress Photoduplication Service #14676.

Kibel, I. A., 1963: Hydrodynamic Methods of Short Period Weather Forecasting. Pergamon Press.

Knighting, E., "Numerical Weather Prediction," See reference 2 above, pp. 478-493.

McClain, E. P., M. A. Ruzecki, and H. J. Brodrick, 1965: "Experimental Use of Satellite Pictures in Numerical Prediction." Monthly Weather Review, 93 (7), pp. 445-452.

Pfeffer, R. L., 1962: "Results of Recent Research in Meteorology at the Lamont Geological Observatory." Proceedings of the International Symposium on Numerical Weather Prediction in Tokyo, pp. 249-263, The Meteorological Society of Japan.

Thompson, P. D., 1961: Numerical Weather Analysis and Prediction. The Macmillan Co.

Thompson, J. R., J. C. Cronin, and R. E. Kerr, Jr., 1964: Silent Area Analysis Using TIROS Data. Aerometric Research Inc., Final Report, Contract No. N189(I88) 57542A.

Todd, J., 1962: Survey of Numerical Analysis. McGraw Hill.

Widger, W. K., Jr., P. E. Sherr, and C. W. C. Rogers, 1965: Practical Interpretation of Meteorological Satellite Data. ARACON Geophysics Co., Final Report, Contract No. AF19(628)-2471.